UNIVERSIDAD CARLOS III DE MADRID

B.Eng. Aerospace Engineering

Final Year Project

Ionic Polymer-Metal Composites: Manufacturing and Characterization

Clara Andrea Pereira Sánchez

This page is intentionally left blank

Acknowledgements

First of all, I thank Instituto IMDEA Materiales for enabling me to use their facilities, labs and resources with the purpose of working out this project.

A special thank to Roberto Guzmán de Villoria, my supervisor and couch in this adventure, who offered part of his intelligence, knowledge and support and whose advices were very important for me to be where I am now.

Thanks to Juan Carlos Rubalcaba for the design and development of the set-up for actuation and the software needed.

Thanks to Vanesa, Marcos and José Luis for helping me a countless number times with their very supportive attitude and smiles in their faces.

Thanks to Manoli for introducing me to the very interesting topic of actuators and making my first days in IMDEA Materiales easier and funnier.

Thanks to Luis and Pablo, who shared a lot of knowledge and ideas with me and showed interest in my results and tests.

Thanks to Alfonso, Jaime, Dani, Marcos, Dani and David for the laughs and interesting conversations every day in the bus ride. And I thank also all the rest of my colleagues in Instituto IMDEA Materiales for the enjoyable moments during the coffee breaks or at the corridors.

In a more personal manner, thanks to my family for showing interest, sharing my happiness, encouraging me to improve and putting up with me when I lose my nerves. Special thanks to my aunt Carmen.

Lastly, thanks to Laura, Nerea, Leti and Guille for always being there. Thanks to Adri and Paulo for being virtually there.

Abstract

This project focus on the investigation of ionic Electroactive Polymers (EAPs) as an electrolyte in the creation of Ionic Polymer-Metal Composites (IPMCs). The polymer electrolyte is coated with a noble metal (gold) and used for the study of actuation, that is, inducing a change in the shape of the material by the application of an electric current.

Firstly a review in EAP actuators is provided, explaining the different mechanisms of actuation, their applications and their potential improvements for future research and work. Later on, it is explained how we built an IPMC and how we implemented actuation in it.

Different techniques were used in order to characterize our material such as Differential Scanning Calorimetry (DSC), Thermogravimetric Analysis (TGA) or Scanning Electron Microscopy (SEM). The material was also subjected to tensile tests in an INSTRON machine to evaluate their strength and Young's modulus.

This work intends to demonstrate a simple and cheap method to build EAP actuators with adequate properties in terms of stress, strain, actuation fatigue life and efficiency for application in some fields as a safer, cheaper and suitable alternative to conventional actuators.

Table of contents

1. Introduction

1.1. Project organization

This project is structured in six chapters followed by a list of references used and the appendices mentioned throughout the report. The chapters which this report is composed by are:

- Chapter 1: brief introduction to the project and its theoretical background.
- Chapter 2: literature review about EAPs, actuators, fabrication processes and experimental data of previous researchers, new challenges regarding material properties of actuators and a rough anticipation of the results that are going to be attained.
- Chapter 3: description of the project.
- Chapter 4: characterization of the material needed for fabrication and preparation of samples.
- Chapter 5: fabrication and preparation prior to the actuation phenomenon.
- Chapter 6: experimental set up and procedures of actuation.
- Chapter 7: conclusion and last observations and recommendations for future work.

1.2. Background

Actuators are used for a wide range of purposes in technology. Going from mechanical moving parts to very high technological applications such as walking robots, prosthetics or in the aerospace field for a more accurate utilization of the flight control surfaces of an aircraft. Effort is being put in the development of new types of actuators to better fulfil the requirements and the safety conditions for these applications. Current challenges for this technology includes safer interaction with humans, energy density optimization, ability to better withstand large forces and lighter devices.

In recent years the investigation in polymers has been augmented due to their potential applications and their exceptional properties when compared to other materials. Their ease to combine with other materials showing pleasing and attractive

properties as well as their high-level compliance in different situations make polymers very attractive materials.

The focus of this project is on polymers that are able to respond electromechanically to specific stimuli. These polymers are also known as electroactive polymers (EAPs). This kind of material has the very interesting property of acting as actuators and sensors: responding mechanically to an electric current or converting mechanical motion to an electric field respectively. There are a great amount of conventional mechanisms and devices that require and are driven by actuators and sets of bearings, gears and other components. However, EAPs are thought to be an alternative to the conventional actuator or sensor in the sense that with a much lower electrical consumption, they show compliant properties such as light weight, considerable shape change, noiseless, fracture tolerant, low power consumption, significant mechanical energy density and so on (Bhandari, Lee, and Ahn, 2012). In *Table 1* some properties of EAPs are compared to other conventional actuators, such as shape memory alloys and electroactive ceramics. A lot of research has recently and is currently being carried out in improving the strain capability, the strength and stiffness of the material, among other characteristics. EAPs are believed to mean a huge advantage in several engineering and scientific fields, thought to be able to create applications and systems that nowadays are just fantasy.

Table 1: Comparison among various actuator materials (Bar-Cohen and Leary, 2000; Shahinpoor, Simpson, and Smith, 1998; Uchino, 1995). *Shape memory alloys produce actuation due to either thermal effect by increasing the temperature or by Joule effect, that is to say that heat is produced as a consequence of current passing through a conductor. This heat induces the shape change and therefore actuation (Kumar and Lakshmi, 2013).

Property	Shape Memory Alloys	Electroactive Polymer	Electroactive Ceramic
Actuation Mechanism	Change of temperature	Electrostatic forces of ion diffusion	Change of phase
Actuation voltage [V]	~5*	Ionic EAP: 1-7 Field-activated: 10-150 V/μm	50-800
Actuation strain	Up to 8%	~300%	0.1-0.4%
Actuation time	s to min	μs to min	μs to s
Density [g/cc]	5-6	1-2.5	6-8
Force [MPa]	700	0.1-25	30-40

1.2.1. State of the art

The origins of the discovery of some polymers being able to behave as actuators or sensors go back to the 1880s. Wilhem Röntgen, a German physicist who first detected electromagnetic radiation in the X-ray range (0.01-10 nm), observed the length variation of a rubber band subjected to an electrical charge. Nineteen years later, in 1899, the first theory on strain response to an applied current was postulated by Sacerdote (Bar-Cohen and Zhang, 2008). However, the first piezoelectric[1] polymer, was not discovered until 1925 thanks to the work of Eguchi (Kestelman, Pinchuk, and Goldade, 2000). This polymer was obtained by solidifying carnauba wax, beeswax and rosin at the same time as a DC current was applied. Some years later, in 1969, Kawai achieved to show the piezoelectric activity of poly(vinylidene fluoride) PVDF (Bar-Cohen and Zhang, 2008). After this discovery, other authors have been investigating on new EAP materials, their properties and their improvement. Since the 1990s the research on EAPs have been mainly focused on biomedical applications as artificial muscles due to the similar motion of the activation phenomenon to that of animal or human muscles.

EAPs can be classified into two main groups based on the method in which they are activated, field-activated and ionic electroactive polymers.

Field-activated EAP requires Coulomb electrostatic forces created by an electric field in between the electrodes on films (Bar-Cohen and Zhang, 2008). Among the field-activated EAPs it is possible to find ferroelectric polymers, dielectric or electrostatically stricted polymers and electrostrictive graft elastomers. They can operate at room-temperature for a relatively long time inducing large actuation forces in a fast manner. However, large strains require high activation fields of values sometimes close to the electric breakdown of the material, which will produce a drop in the material resistance and thus the transition of the material to a conductor (Ieda, 1980).

In contrast to field-activated EAPs, ionic EAPs produce the actuation phenomenon by transport or diffusion of ions within the material membrane. Normally the actuation comes in form of bending of the material at low voltage and activation energy. They

[1] "The direct piezoelectric effect is present when a mechanical deformation of the material produces a proportional change in the electric polarization of that material, i.e. electric charge appears on certain opposite faces of the piezoelectric material when it is mechanically loaded" (Gautschi, 2002).

require two electrodes and an electrolyte to function. Nevertheless, some of the major drawbacks they are characterized by are low durability and efficiency, slow response as ion diffusion takes longer to occur and, normally, relatively low stiffness and blocking force[2] (Tiwari and Garcia, 2011).

Advances are needed in the field for increasing the response to the electrical current, expanding lifetime and their performance in general to make them suitable for important industries such as the biomedical, electrical, electronical, aerospace, mechanical or textile, among others.

1.3. Objective

In this project we are going to build an actuator from an ionic EAP. This kind of actuators in comparison to others are lighter and simpler to build and use. Good overall performance as artificial muscles and the possibility of implementation in robotics as a safe alternative to conventional mechanical actuators is another reason to chose this material, though more investigation is needed in the topic.

We are going to design and build an Ionic Polymer-Metal Composite (IPMC) actuator composed by a polymer membrane capable of ion exchange in aqueous media and two metal electrodes coating both faces of the polymer membrane. This material is going to be mechanically and electrically characterized to observe the properties influencing the actuation process and understand the principles behind it. Finally, the actuation mechanism in going to be observed and tip deflection in a cantilever configuration is going to be measured as a function of the electric field passing through.

[2] Blocking force or generative force is the maximum force exhibited by the tip of a bending actuator in a cantilever beam set up with showing no displacement (Yun, Kim, and Kim, 2008).

2. Literature review

This chapter starts with a general review of what an Electroactive polymer (EAP) is, explaining the two different types of EAPs based on the actuation mechanism they are driven by. Examples of materials from each classification are also provided. Later sections on this chapter include an overview of applications where EAPs have been shown to be useful and mean a huge advance in science and technology. To end with, the actuation mechanism of EAPs is going to be explained and compared to prior technologies.

2.1. Electroactive polymers (EAPs)

Electroactive polymers are materials, as aforesaid, that are shown to be able to behave as actuators and sensors because of their ability to respond mechanically to electrical stimulation. Their operational resemblance to animal muscles and other natural tissues by exhibiting large strains when subjected to an electrical stimulus have positioned the investigation on EAPs as target in many scientific fields, as well as their properties and the potential improvements on them. In comparison to other inorganic materials, EAPs present several attractive properties such as lightweight, easy to manufacture, large strain when exposed to an electric current, etc. Electroactive polymers can be classified in two different groups attending their type of actuation: field-activated and ionic EAPs.

2.1.1. Field-activated EAPs (FEAPs)

Field-activated or electronic EAPs are a type of electroactive polymer that shows dipole formation and Coulomb interaction when an electric field is applied. One of their main features, apart from their high efficiency, is the fast response speed, which indeed is determined by the polymer dielectric and the elastic relaxation time. Strain can be visible as a reaction to the electric current in various scales: macroscopic, microscopic and molecular. The conformation of the latter can be changed when applying a voltage

as the dipoles within the polymer arrange with the direction of the current (Bar-Cohen and Zhang, 2008).

Field-activated EAPs are light, easy to manufacture and manifest high flexibility and impact resistance. Examples of field-activated EAPs are PVC, PVDF and silicone, among others. Most of these kinds of electroactive polymers are actually widely used in daily life for insulators or coatings but they can also be thought to produce electroactive molecular devices in the nano and microscale (Cheng and Zhang, 2008). In most cases, due to their high glass transition temperature[3] T_g, they are inadequate for low temperature actuation (below the T_g of the material) as it would be the case for artificial muscles or room temperature applications. In *Table 2* some field-activated EAPs' T_g are specified. The higher the T_g, the narrower the temperature range in which actuation occurs because the material can only change size or shape with a temperature beyond its T_g (Harwin et al., 2004). The ideal case for an actuator would therefore be a low T_g material with high molecular mobility.

Table 2: Data for glass transition temperature T_g for different field-activated EAPs (Scott, 2001). Actuation to be efficient should occur at higher temperature than the T_g. Most of these materials are therefore inefficient at room or low temperature and thus not suitable either for biomedical engineering applications.

Material	Glass Transition Temperature T_g [ºC]
Polyvinyl chloride (PVC)	80
Polyvinylidene fluoride (PVDF)	-35
Polyamide (Nylon)	50
Poly(chlorofluoroethylene) P(CFE)	45

Field-activated EAPs can be sometimes difficult to classify and authors offer different ways of classification. Cheng and Zhang divided them into four categories: piezoelectric, electrostrictive, electrostatic and electrets-based (Cheng and Zhang, 2008). In the following lines each of these types are going to be briefly described.

- *Piezoelectric and ferroelectric EAP*: the ferroelectric effect is a property of some materials that present spontaneous electric polarization that can be reversed. Spontaneous electric polarization is a phenomenon that is

[3] Temperature below which a polymer has a hard and brittle behaviour. Above the T_g polymers become rubbery, soft and flexible. The T_g is a second order transition, which means that it involves a change in the heat capacity of the material but not in latent heat.

characterized by parallel orientations of electric dipole moments in the absence of an external electric field.

To obtain piezoelectrics from ferroelectric materials it is needed a change in the polarization of the material. This process is known as poling, and it consists of an electric current passing through the material, causing the development of its spontaneous polarization and the single direction alignment of its dipoles (see *Figure 1*) (Shaw, 2014).

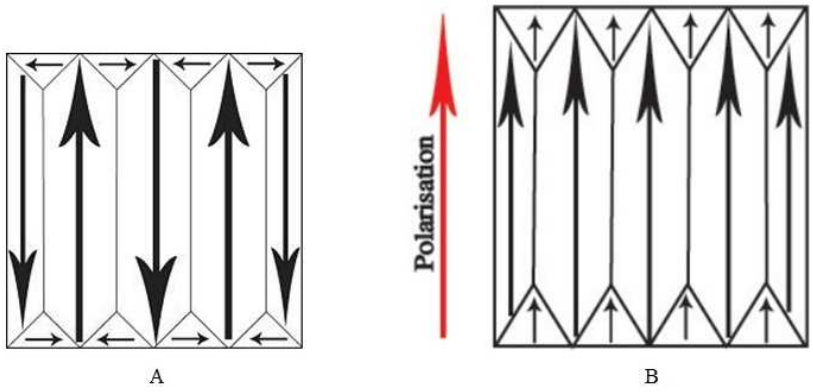

Figure 1: In A, a ferroelectric material with its spontaneous dipole orientation. In B, the piezoelectric material obtained from the ferroelectric by poling .In the poling process an electric current is passed through the ferroelectric material, changing its spontaneous polarization and aligning all its dipole moments to the same direction (Shaw, 2014).

If stress is applied to a piezoelectric material, as in *Figure 2*, an electric current is generated. Polymers in this category are normally present in semicrystalline form, and their crystallites are enclosed to an amorphous surrounding.

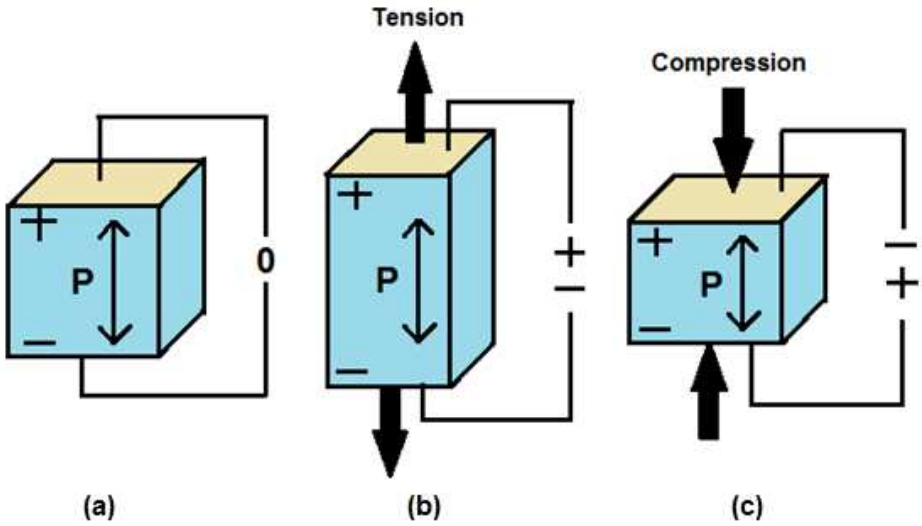

Figure 2: Piezoelectric material as a current generator. (a) shows the piezoelectric material with no current supply and no strain applied. If a tension force is exerted to the material as in (b), an electric current appears on the surfaces of the crystal. Polarity of this current can be changed by inverting the force to a compression, as in (c) (Vatansever, Siores, and Shah, 2012).

Some examples of piezoelectric EAPs are PVC, PVDF or P(VDF-TrEE) copolymer (NASA, 2014). This latter one is shown to behave with the largest electromechanical response at room temperature, which is important for artificial muscles and biomimetics applications (Cheng and Zhang, 2008). Yet piezoelectric EAPs, although they manifest low power consumption, have very high stiffness and low strain abilities (~0.1%) for many applications at low frequency or large impact excitations (Cottinet et al., 2004)(Goulbourne, 2005).

- *Electrostrictive EAPs*: these polymers have withstood strains of up to 30% and pressures up to 1.9MPa and are based on the principle of dipole density variation in a material. For polymers that are isotropic, polarization in one direction produces an extension in the perpendicular direction and a contraction in the parallel, shown in *Figure 3* (Cheng and Zhang, 2008).

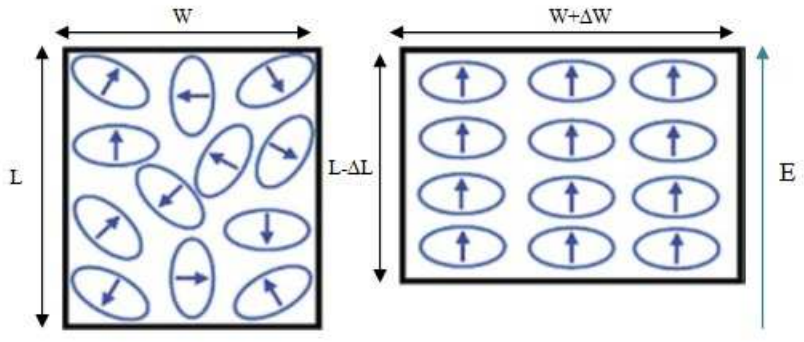

Figure 3: On the left, a material with spontaneous polarization in the absence of an electric field. Electric dipoles are randomly oriented. On the right, an electric field is applied on the material and subsequent rearrangements of electric dipoles occur, and as a result, shape changes take place (Adapted from Cheng and Zhang, 2008).

Electrostrictive polymers present a general performance similar to those of biological muscles. Though it is not the best performance when compared to other actuator technologies, it is the one that, in general, matches muscles properties and functions accurately. For instance, silicone was reported to have a strain close to 32%, 0.21MPa of maximum pressure, and a maximum energy density of 0.034 J/cm^3, whereas the same values for muscles are >40%, 0.35MPa and 0.07 J/cm^3(Kornbluh et al., 1998).

- *Electrostatic force EAPs or Maxwell stress polymers*: among which dielectric elastomers stand out, can be sustained to strains proportional to the square of the electric field applied (Goulbourne, 2005). These polymers are formed by a soft dielectric elastomer between two electrodes. An electric field passing through the elastomer polarizes it and generates a stress within the dielectric material called Maxwell stress. The dielectric material tights in directions parallel to the force and stretch in the directions perpendicular to it (Goulbourne, 2005). To differentiate it with electrostrictive EAPs it is necessary to bear in mind that the square of the electric displacement in the latest is proportional to the strain, whereas in electrostatic EAPs this is not true (Cheng and Zhang, 2008). This is because the origin for electrostriction falls on an atomic or molecular level while the Maxwell stress effect is an elastic event.

  Elastomers are obtained by the vulcanization of polymers with a non-crystalline structure and heating with sulphur, traditionally. Their properties depend highly on its cross-linking level.

Electrostatic elastomeric EAPs, such as silicone rubbers, operates at high voltages of MV/m and are capable of resist very high strains even above 100%. Wide operating temperature range (-100ºC to 250ºC) and low vibration and noise are other advantages. The efficiency of this materials is estimated to 80-90% at actuation rates of 1-20Hz assuming charge recovery (10-50% without charge recovery) (Pelrine, Kornbluh, and Joseph, 1998; Goulbourne, 2005). However, low stiffness is a problem when considering structural or mechanical applications that need to withstand certain weight.

- *Electret-based EAPs*: arose as a combination of the dielectric properties of elastomers actuators and the high bipolar nature of electrets[4]. They became of high importance because of its applications as microphones, speakers, transducers and so on. They are normally composed by an electrets diaphragm next to a pierced metal plate and separated by some spacers, as can be seen in *Figure 4*. Some advantages they present are simplicity in construction, high efficiency and frequency response (Ko et al., 2012).

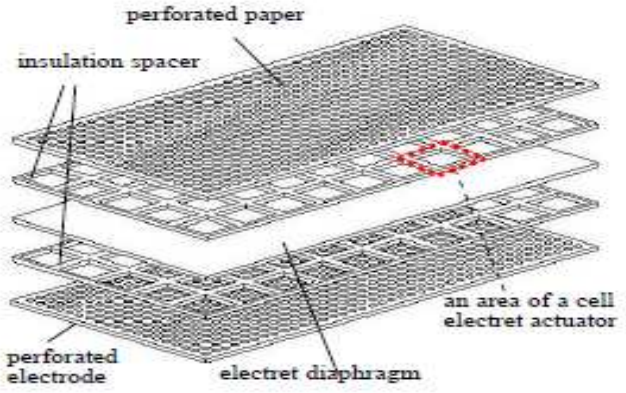

Figure 4: EAP configuration for loud-speaker application. The typical layers of an electrets-based EAP are shown: electrets diaphragm covered by spacers and perforated electrodes (Ko et al., 2012).

2.1.2. Ionic EAPs (I-EAPs)

Since the 1960s, ionic EAPs have been used in proton exchange membrane fuel cells but it was not until the 1990s that researchers found the actuating and sensing

[4] An electrets its "a dielectric material that conserves a permanent electric polarization after an external field vanishes, and that plays in electrostatics the same role as permanent magnets in magnetostatics"(Lévy, 2008).

capabilities of this kind of materials. Proton exchange membrane fuel cell produces electrical energy as a result of a chemical reaction between hydrogen (anode) and oxygen (cathode) instead of a direct combustion of both gases to deliver thermal energy (J. S. Lee et al., 2006). The membrane must be able to let the hydrogen protons from one electrode through but not the electrons, which induces a current that reacts with the oxygen of the other electrode to create water, as pictured in *Figure 5*.

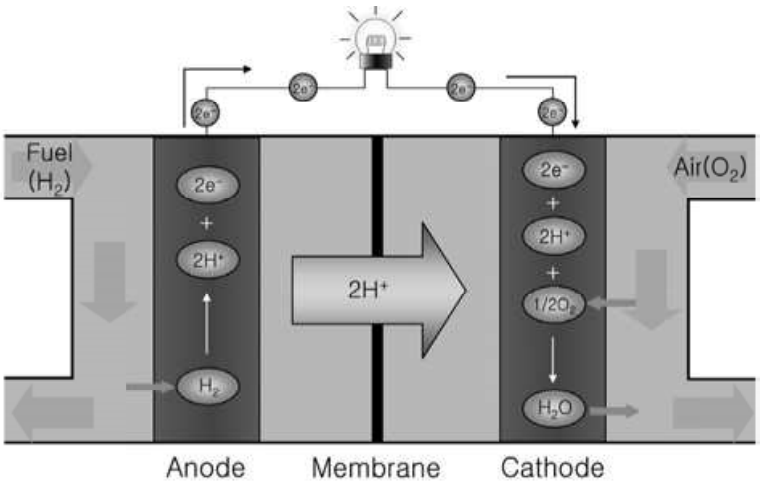

Figure 5: Operational scheme of PEM fuel cells (J. S. Lee et al., 2006).

In the case of ionic EAPs, diffusion or mobility of ions within the polymer membrane is the basis for actuation, which can be obtained at lower voltages than field-activated EAPs, though it is difficult to maintain a constant strain during a certain period. They normally need to be formed by an electrolyte, coated in both surfaces by electrodes, what is known as Ionic Polymer-Metal Composite (IPMC). Ion diffusion appears from two different origins: aqueous electrolyte or ionic liquid electrolyte, being these lasts preferred as they present very low vapour pressure, operation voltages and are extent of the hydrolysis exhibited in aqueous systems. Various materials can be used as electrodes such as carbon or metals (noble metals i.e. Pt or Au, as in this case) (Bhandari, Lee, and Ahn, 2012) (Hong, Almomani, and Montazami, 2014). In *Figure 6* an example of an Ionic EAP is shown.

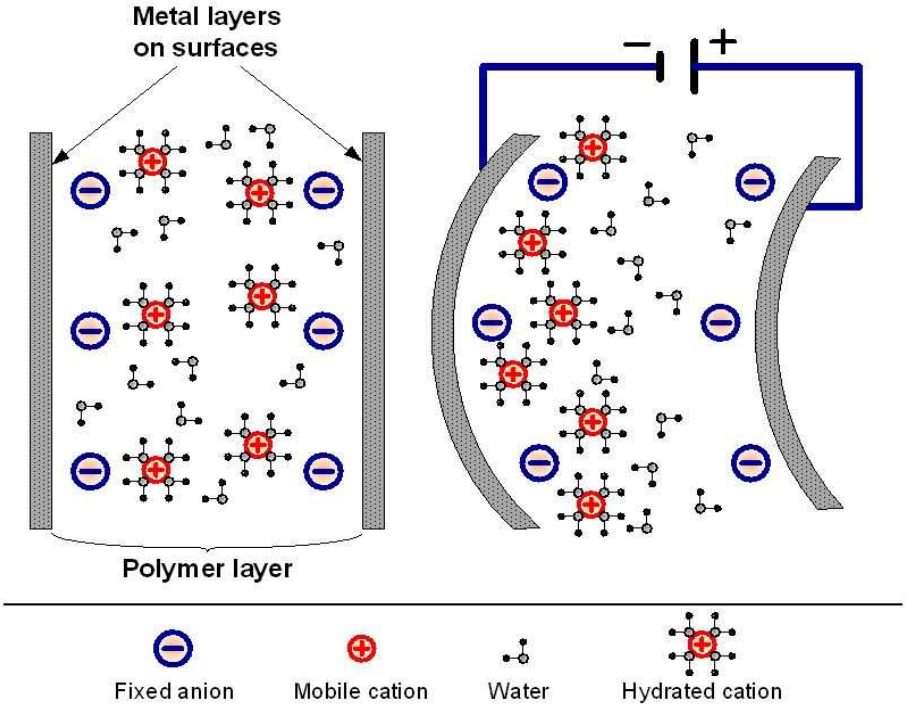

Figure 6: Example of ionic EAP actuator of IPMC (Doam and Ahn, 2012). Left: in the absence of an electric field, the material's ions are randomly distributed within the polymer layer. Right: when a current is applied to the metal surfaces, cations are shifted towards the anode and bending occurs.

Whereas field EAPs change size or shape when actuating, ionic EAPs response is an anisotropic volume alteration, triggering the bending of the material, as can be seen in *Figure 7*. In other words, when subjected to an electric field, the accumulation of anions and cations at the oppositely charged electrode produces an asymmetric change of volume on the polymer which bends the IPMC. This is because of the considerably smaller size of anions compared to cations. As a result of this, the actuator bends towards the anode (Hong, Almomani, and Montazami 2014).

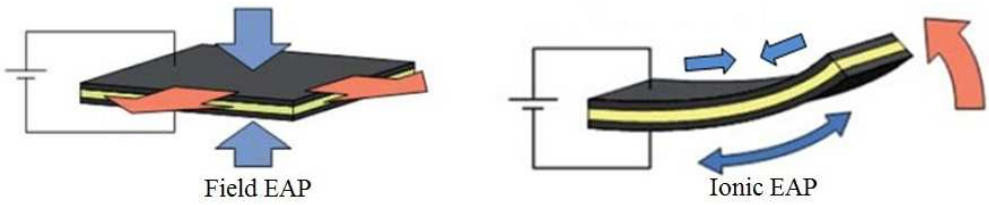

Figure 7: Comparison between a field EAP and an ionic EAP (Adapted from MacFarlane et al., 2014). On the left an example of field EAP actuation : the material expands (red arrows) as a result of an electric field applied. The intrinsic force created when actuating (blue arrows) compress the material. On the right, an ionic EAP actuation: intrinsic forces (blue arrows) provoke the material bending (red arrow) towards the anode due to a differential in length of both electrode layers.

Among ionic EAPs, one can find ionic polymer gels, conductive polymers, ionic polymer-metal composites (IPMC) and carbon nanotubes.

- *Ionic polymer gels:* are cross-linked polymers dispersed in water that may or may not be reinforced. (Calvert, 2008).

  Gels actuating mechanism can be driven by different factors, as we will see in the following lines.

  Electrically driven actuators are formed by two electrodes that are placed in a salt solution, producing hydrolysis, generating hydrogen on the cathode (decrease of pH) and oxygen on the anode (increase of pH). Due to this differential in acidity, some gels will enlarge, shrink or bend. This kind of gels, however, has not provided good results for stiffness and actuation rate.

  The gels activated thermally normally show a quick switch from the enlarged state to the shrunk one when temperature rises. They present small values for Young's modulus.

  Chemically driven gels produce good force and strain capabilities when subjected to pH variations. Although actuation time is quite large compared to biological muscles, they quite resemble to them. Other types of gels are being catching scientists interest in the last few years, although their classification as I-EAP is not clear yet: oscillating reactions (by periodic redox reactions of the material, *Figure 8*) and electro- and magnetorheological driven gels (Calvert, 2008).

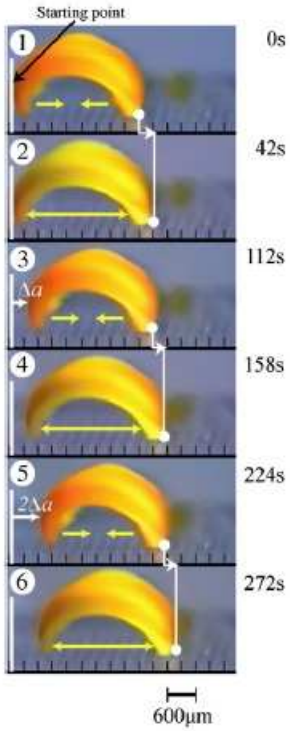

Figure 8: Motion of a self-oscillating actuator immersed in a solution (R. Yoshida et al., 2009). Actuator behaves as a worm, the front edge can move forward when elongating (due to oxidation) while the rear one stays still, and the other way round when reduction takes place: the rear edge moves forward while the front one is prevented from sliding. The backwards motion of each edge is prevented by a saw surface at the bottom. For the asymmetrical swelling of the actuator a hydrophilic acid is copolymerized into the polymer.

- *Conductive EAPs*: it has also been investigated the possibility of employing conductive polymers. In response to an applied voltage, these polymers swell due to a red-ox reaction, depending on the polarity, as explained as well in *Figure 9*. Thus, it causes inclusion or removal of ions that are solved. The first conductive EAP was polyacetylene, which conduction properties are derived due to the existence of alternating C-C double bonds on the polymer backbone followed by ion doping. However, polyacetylene is not useful as an actuator. For this purpose, other conductive EAPs have been explored and synthesised (Pillai, 2011). Some examples are polypyrrole, polyaniline or polythiophenes.

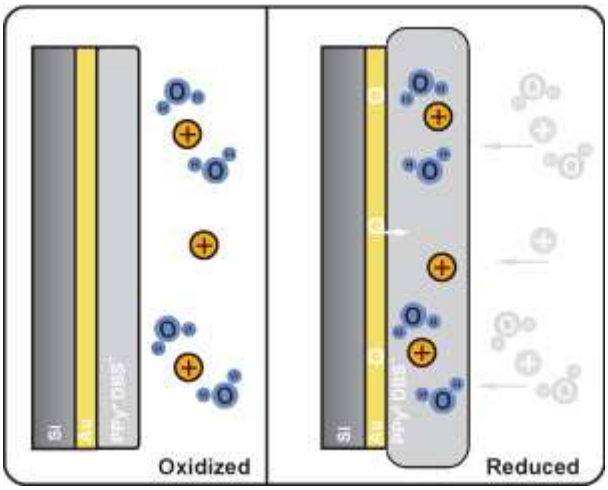

Figure 9: Schematic of a conductive polymer actuator (McGill University, 2014). On the left the conducting polymer, in this case polypyrrole, is not actuating. The material is submerged in an electrolyte solution in the presence of ions. When a current is applied to the material, these ions are attracted to the polymer and get into it producing a volumetric expansion.

In order for conductive EAPs to be useful for actuation they need to be stable in air as a bulk material. Physical properties of the material (electrical conductivity, porosity, dopant ion...) or chemical properties of the environment (ion concentration, temperature, electrolyte...) are determinant for the material strain capabilities (Pillai, 2011).

- *Ionic polymer-metal composites (IPMC):* these are materials formed by two metallic electrodes sandwiching a polymer electrolyte. Normally, the material needs to be hydrated to perform actuation, which occurs in the form of bending. This type of actuator is going to be further explained in section 2.2, as it is the focus of this project.

- *Carbon Nanotube based actuators (CNT-based actuators):* CNTs by themselves are not ionic EAPs and cannot work as actuators. Nonetheless, CNTs can be mixed and processed together with other EAPs. In this way the strain capabilities of these polymers are coupled with the outstanding properties of CNTs, making evident some improvements in actuation in terms of stress generation. Actuation mechanism for this kind of actuators is generated by different factors: double-layer charge injection and photothermal or electrostatic actuation. In recent years, CNTs have been

mixed with other EAPs in order to improve actuation performance of material characteristics (Kosidlo et al., 2013), as *Figure 10* shows.

Also studies were carried out to compare actuation and electrochemical properties of an actuator using the same bucky gel electrolyte as in *Figure 10* but varying the electrodes using Single Walled Nanotubes (SWNT)/Ionic Liquid (IL)/polymer electrode, SWNT/IL electrode or a simple gold coating electrode by Terasawa and Takeuchi. Results concluded that electrodes using SWNT/IL performance when actuating was superior for low voltage applications.

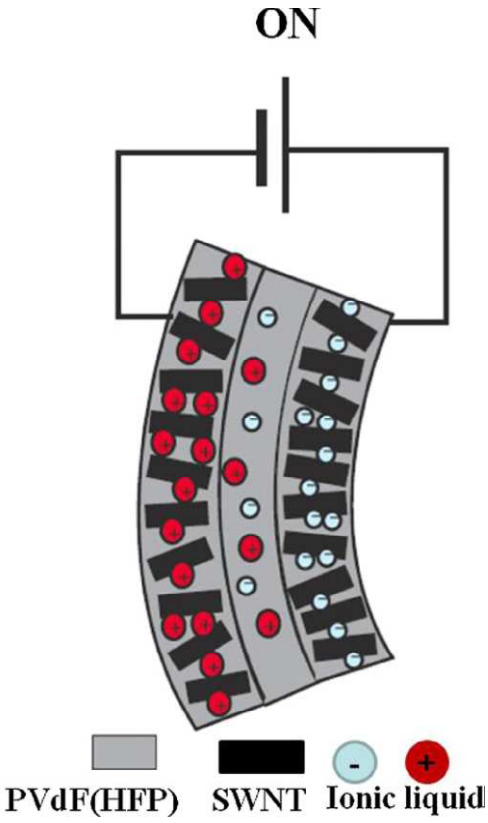

Figure 10: EAP actuator formed by a poly(vinylidene fluoride-hexafluoropropylene) PVdF(HFP) electrolyte and two polymer-supported bucky-gel electrode layer with single walled nanotubes in the presence of ionic liquid (Terasawa et al., 2011). When the actuator is connected to an electric field, ions in the gel electrolyte layer are transferred to the anode and cathode and thus create a double layer with negatively and positively charged nanotubes. Swelling occurs in the cathode layer while the anode layer shrinks, leading to the actuator bending.

As another example of using ionic EAPs with CNTs, studies have also reported the electromechanical performance improvement arose when implementing Vertically Aligned CNTs (VA-CNTs) as a conducting

network composite electrode (Liu et al., 2010). A picture showing this structure can be seen in *Figure 11*. The advance in actuation came due to the fast ion conduction through parallel channels created in between the VA-CNTs and the decrease of electrical conduction resistance.

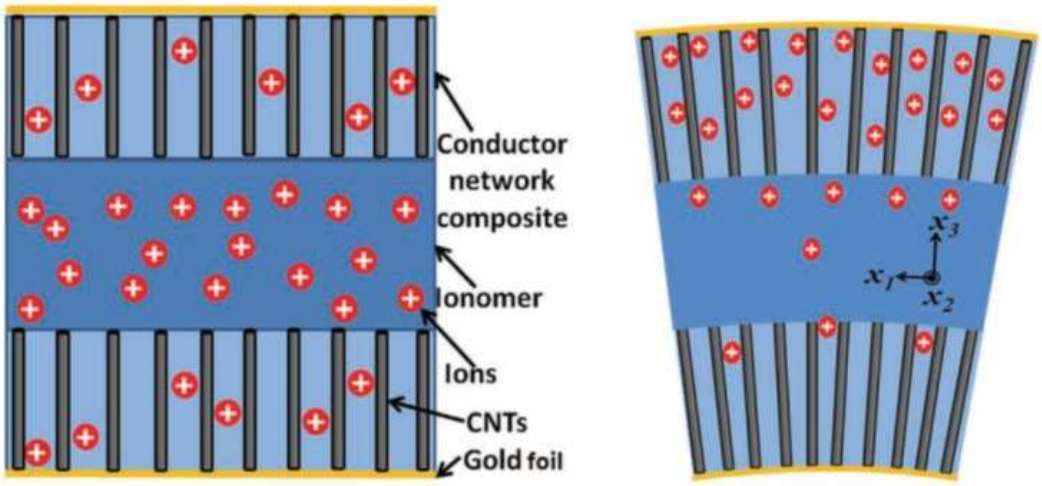

Figure 11: Scheme of an actuator formed by VA-CNTs within the conducting network composite layers as electrodes (Liu et al., 2010). On the left, an actuator with no voltage applied. On the right, a bent actuator with a voltage applied showing the mobility of cations with respect to the previous one.

In *Table 3* some important typical values for actuation are summarized according to Madeen and Bennett (J. D. W. Madden et al., 2004; Bennett and Leo, 2003) for most of the types of EAPs described above. As can be seen by looking comparatively the data, electrostrictive polymers can be a very good option for an actuator material, as its strain capabilities are outstanding, if no stress need to be withstood by the structure. Although CNT-based EAPs can sustain bigger stresses, their efficiency is low as stiffness is increased due to the presence of the CNTs. According to the data listed here, IMPCs present adequate strain and stress capacities coupled with high number of cycles until failure. These properties together with low operating voltage, low energy consumption, and safety when implementing them, make IMPCs suitable and recommended for most applications, including artificial muscles.

Table 3: Mechanical properties of several EAPs.

Property	Piezoelectric	Electrostrictive (silicone)	Conductive Polymer	IPMC	CNT-based
Max. Strain [%]	3.5-7	120	12	3.3	~1
Strain rate [%/s]	2,000	34,000	1	3.3	0.6
Density [kg/m^3]	1,870	1,100	-	1,500	230
Max Stress [MPa]	45	3.2	34	15	27
Life [cycles]	-	10^7@5% strain	28,000	250,000	-33% strain after 140,000 cycles

2.2. Ionic Polymer-Metal Composites (IPMCs):

The focus of this project is to develop an IPMC actuator. Due to their light weight, strain abilities and low driving voltages when actuating, IPMCs are believed to mean great advantages in the future of material science applied to bioengineering. In general, an IPMC is formed by a polyelectrolyte membrane, such as Nafion or Flemion, covered in both faces by an electrode (see sketch in *Figure 12*), which used to be a noble metal (Au, Pt, etc) (Bhandari, Lee, and Ahn, 2012).

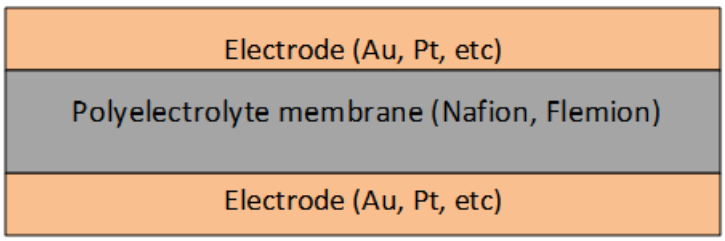

Figure 12: Simplified sketch of an IPMC material composed by an electrolyte membrane coated in both sides with noble metals serving as electrodes.

These polyelectrolyte membranes present ionisable groups covalently bonded to their backbone structure, as can be seen in *Figure 13*, that allow specific ions to pass through while impeding others diffusion. In turn, the large polymer backbones determine their mechanical strength.

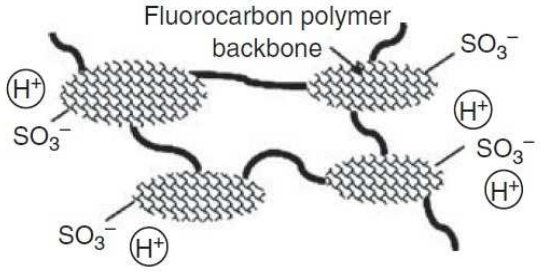

Figure 13: Scheme of a fluoropolymer chain with ionisable groups SO_3^- and H^+ (Park et al., 2008).

In a dry state, cations are not able to move since they are cross-linked to polymer chains. Nevertheless, in hydrated conditions, cations are surrounded by water molecules, enabling their mobility *(Figure 14)*. For this reason, normally IPMCs are submerged into liquids or used along with ionic liquids for efficiency improvement. Thus, when an electric field is applied to the material, associated electrostatic interactions provoke the IPMC material to bend towards the anode.

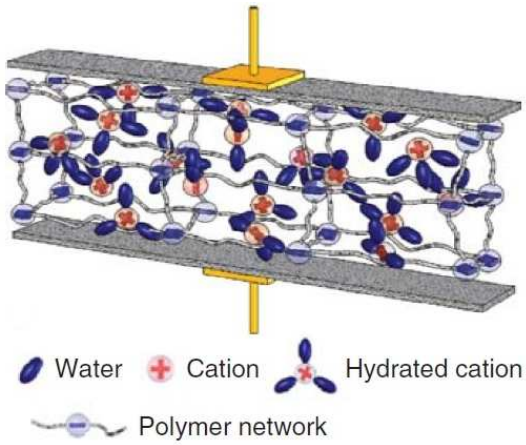

Figure 14: Scheme of a structure of an IPMC in a wet media (Park et al., 2008). Water molecules surround cations that were previously joint to the polymer backbone and enable them to move through the membrane.

For electroding the membrane surfaces, chemical processes are ideally preferred due to their better adhesion but in turn they are normally more expensive. A more simple and fast way for plating the IMPCs is mechanical electroding, including techniques as solution casting, physical vapour deposition method as sputtering or direct manufacturing. Sputtering has indeed showed better performance in tip displacement and force though they are subjected to surface deterioration (Tiwari and Garcia, 2011).

When alternating voltage is applied, each time the voltage is reversed so is the bending direction. The distance the tip deflects in a cantilever configuration (see *Figure*

15) does not only depend on the voltage but also on the frequency it is changed if alternating voltage is considered. The smaller the frequency, the higher the displacement from the original position (dashed line in *Figure 15*) can be, until a critical value is reached.

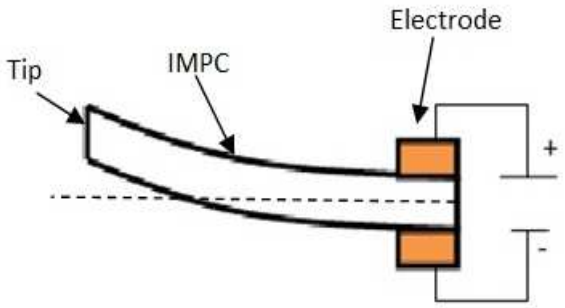

Figure 15: IPMC actuator scheme showing a cantilever configuration. In the fixed side an electric current is applied directly to the electrode layers while the other side is free to move.

Interesting characteristics also arise for IPMC in static test results in terms of displacement and blocking force, as they act much alike composite beams. The blocking force is the maximum force exerted by the actuator when its displacement is completely blocked, i.e. force needed to be applied to an actuator at a given voltage in order to come back to their equilibrium position (at 0V).

One of the main disadvantages of these EAPs is that bending relaxation occurs due to water diffusion out of the areas where more cations are present. Another one is low blocking force (Tiwari and Garcia, 2011).

When trying to overcome these drawbacks, several scientists have tried with using ionic liquid instead of an aqueous medium and obtained higher stability but slower response (Hong, Almomani, and Montazami, 2014). Also, making specimens thicker, addition of uniformly distributed multi-walled carbon nanotubes (Lee et al., 2007) or filling the polymer matrix with materials that provide additional cations to the membrane such as montmorillonite or modified silica was tried to improve the blocking force (Nguyen, Lee, and Yoo, 2007). Improvements in the bending response arose by optimizing the IPMC fabrication (metal reduction, surface treatments and so on).

2.3. EAP applications

Electroactive polymers have been studied in the past decade as a state-of-the-art material to produce artificial muscles and develop robots inspired in nature that are able to walk, swim, fly or dive as animals or humans can do. Nevertheless, those are just a few applications of what EAPs can be used for. Thanks to the exceptional properties of some EAP materials which include fracture tolerance, resilience or similarity to biological muscles, some other areas are being investigated. Toys, power generators, smart structures, noise isolation, electronic and optical devices and industries such as the biomedical, the aerospace or the automotive are investigating in how to implement and take advantage of EAP materials characteristics.

Beginning with nature inspired robots, a jellyfish robot using an IPMC composed by a fluoropolymer electrolyte was developed in 2009 taking into consideration the motion of this animal as well as the fluid vortices that characterized jellyfish' diving. Thrust came for the body shape change from an elongated shape to the normal bell shape of the jelly fish. This shape change was imitated using IPMC actuators as can be seen in *Figure 16* (Yeom and Oh, 2009). Other swimming animals have also been reproduced such as fish, corals or eels (Shahinpoor, Simpson, and Smith, 1998; Shahinpoor, 1991).

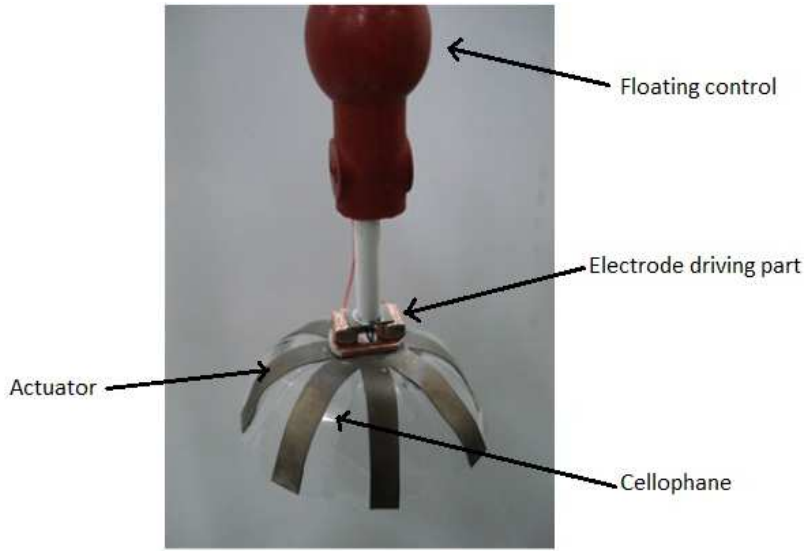

Figure 16: Jellyfish robot (Adapted from Yeom and Oh, 2009)using curved IMPC actuators separated from each other as the jellyfish' arms. Cellophane was used to prevent a decrease in thrust due to water leakage in between the actuators. All actuators are connected to the electrode driving part, providing in this way an in-

phase actuation. On top, a balloon was used in order than the buoyancy of the jellyfish is controlled by adjusting the air to water ratio.

Birds, flies and other flying animals have also been imitated using actuators. Flapping actuators are thought to transfer the bending deformation to the wing (see *Figure 17*) and actuation comes because of the first natural frequency, which can be varied to optimize flapping angle or flapping frequency. Attained results showed that a flapping angle of 85º can be achieved at low frequencies of 3-4V at 0.5Hz (S. Lee et al., 2006).

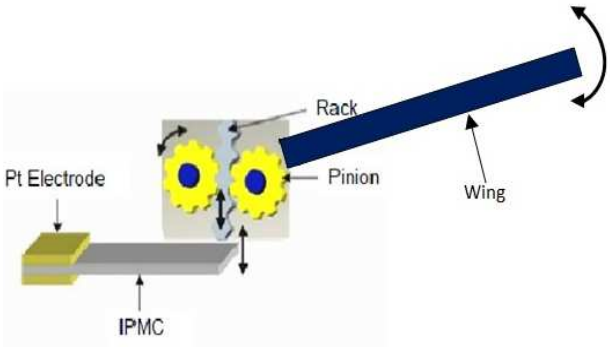

Figure 17: Scheme of a flapping mechanism driven by and IPMC actuator that resembles flying animals wing motion (Adapted from S. Lee et al., 2006). Actuation of the material moves a rack up and down. This motion is transferred to pinions that rotate and consequently move a wing attached to them amplifying the 'flapping' angle.

Several EAPs have been case of study for applications in motors and combustion engines that produce propulsion, rotation, pressure application, etc. The main aim for the utilization of these relatively novel materials are the accuracy of functioning at high frequencies and the ease of place in an precise position, as happens for example with piezoelectric EAPs.

In the work of Madden et al., a case study is shown of how EAPs can be employed to design a variable propeller blade for an Autonomous Underwater Vehicle (J. D. W. Madden et al., 2004). In the naval industry, variable pitch propeller blades are used for cases where vessels may function in several different flow situations. The main aim of this work was to study the possibility of changing the gears that activate the camber and pitch variation of the blade by EAPs. After a comparison of the properties between the EAPs they were considering and the conditions they are require to withstand, such as temperature, strain or stress, they concluded that electrostrictive, piezoelectric and

conducting polymers actuators can be a possible solution to implement (Madden et al., 2004). The same principle can be however employed for any blade where variable camber (see *Figure 18*) can be useful due to the fluid dynamics principles governing the motion or application of the propeller, as can happen for aviation propellers or plane wings for deflection of high lift devices.

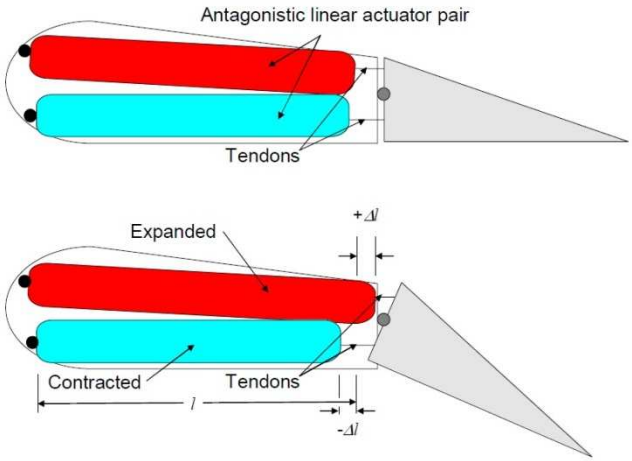

Figure 18: Scheme showing the application of linear actuators to the deflection of the trailing edge of a foil (J. D. Madden, 2004). An actuator pair is connected to the movable trailing edge by tendons which are in charge of transferring the actuating motion. An oppositely actuation (i.e. one actuator expands while the other shrinks) produces a length increment differential Δl and –Δl that induces the trailing edge deflection.

When coming to the space field, EAPs have been also research for applications where demand is sometimes tough and reliability is a major requirement. These applications include a dust wiper for a robot (in *Figure 19*), a gripper or a robotic arm lifter (Bar-cohen, 2004) that are useful for terrain sample acquisition in other planet surfaces. However, for improving the performance of these objects, there is still the need of increase the actuation force and withstand adverse ambient temperatures such as very high and very low temperatures or vacuum pressure over a long period of time.

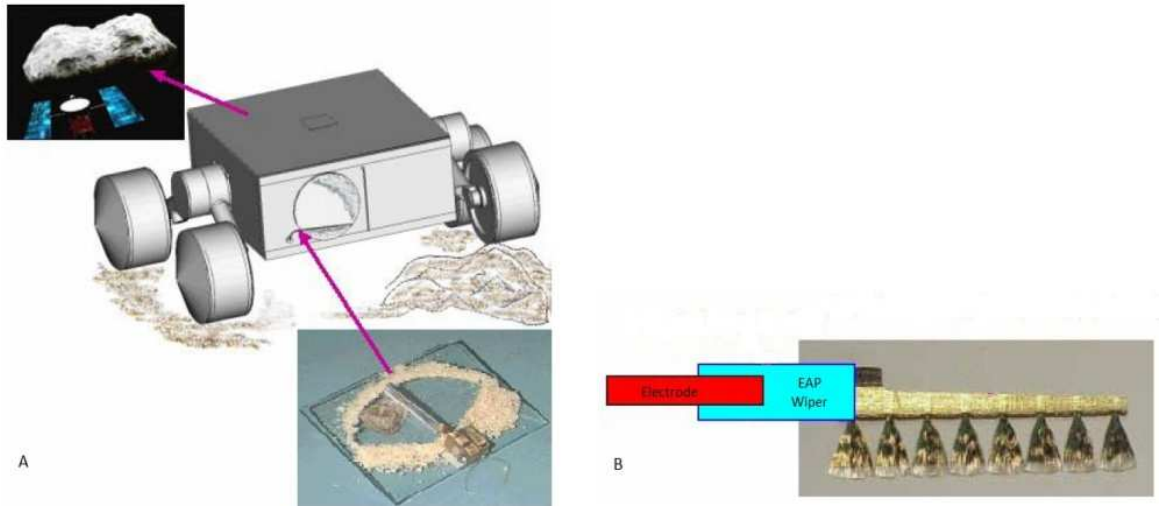

Figure 19: EAP actuator for application as dust wiper for planetary applications (Bar-cohen, 2004). In A the scheme of the dust wiper nano-rover is depicted with the location of the dust wiper specified. In B the EAP dust wiper structure composed of an electrode in contact with the EAP material, which drives the dust wiper.

EAP materials can be useful for many applications and objects, some of which have been explained. They can mean a huge advantage in several aspects of technology and progress. For certain purposes, they can provide advantages over usual hydraulic or mechanical actuators in the sense that they require small operating voltages and eliminate the necessity of moving parts. Nevertheless, more study is required to better understand EAPs actuating and sensing mechanisms and to improve EAPs characteristics and develop suitable structures.

3. Project aim and description

The aim of the project is to develop an actuator with easy and low-cost processing techniques with the novelty of using no ionic liquid or solvent within the polymer membrane. Although actuation is not enhance by adding these substances, the material is not dried before manufacturing the actuator to permit the mobility of ions. No surface treatment is applied after the gold sputtering also with the aim to minimize costs.

We are going to build an ionic EAP actuator of IPMC type formed by a fluoropolymer electrolyte membrane processed as a layer with a hot-plate press and coated in both sides with gold, which serve as electrodes. The electrodes are deposited by sputtering.

Some prior tests and characterization are important to determine material properties that will determine the processing of the actuator, such as Differential Scanning Calorimetry (DSC) or Thermo-gravimetric Analysis (TGA). These results are important to select the conditions for the processing of the material in layers, as is going to be covered in other coming sections of this report. In order to be able to shape the material from pellets and control the thickness, a temperature higher than the T_g has to be attained.

A low weight IPMC is obtained and specimens are cut out from the IPMC layer for characterization and also for actuation. Even though the processing techniques are not improving actuation or mechanical properties, we are going to prove that this material is eligible as a low cost actuator with suitable properties.

3.1. Fluoropolymer: state of the art

The chosen fluoropolymer is a poly(tetrafluoroethylene) ionomer with sulfonic acid ($-SO_3H$) side chains. Its application have been focus of study during the last decades because of its chemical and thermal resistance, as can be found in most fluoropolymers, and also because of its mechanical strength, ion-exchange and water adsorption

capacities (Perma Pure LLC, 2014). Further information about the chemical characteristics of the material can be found in *Appendix I.*

Because of this reason, this kind of polymers exhibit very high chemical and corrosion resistance and they do not normally dissolve in solvents (Zeus Industrial Products Inc., 2006).

The sulfonic acid group anchored to the fluoropolymer attributes some special characteristics as the ability to operate as an exchange membrane within solutions, to absorb water both in liquid or vapour state and, furthermore, to function as a catalyst for many chemical reactions because of its strong acid nature.

Numerous studies regarding the microscopic and nanoscopic structure of fluoropolymers have been made using several techniques. Results gave a wide number of different explanations and theories regarding the material structure. Very recent studies present some fluoropolymers as materials composed by ionic clusters of 5-30nm separated by wide channels of 0.3-0.88nm long. Clusters increase their size when hydrated, although the total number of clusters is seen to be diminished (Gebel and Moore, 2000; James et al., 2000; Gebel, 2000; Orfino and Holdcroft, 2000). Nevertheless, it is still unclear the shape or configuration of these clusters.

Other studies were able to illustrate the water or ion liquid absorption properties of fluoropolymer membranes. The most supported idea was that hydration of the fluoropolymer molecules strongly depends on temperature. The higher the temperature, the more hydrated the membrane would be and the higher the mobility of ions within the membrane (Boyle, McBrierty, and Eisenberg, 1983). Also, when cooling, a new thermodynamic equilibrium will be set because of a change in vapour pressure. In DSC studies, endothermic peaks showed the melting point of water at temperatures close to 0ºC and lower for smaller water content, whereas exothermic peaks, higher with bigger water content, showed water crystallization in the membrane (Yoshida and Miura, 1992; Pineri, Volino, and Escoubes, 1985).

The fluoropolymer used is a polymeric material that exhibits viscoelastic behaviour, that is, viscous and elastic characteristics when undergoing deformation. Viscoelastic materials respond with energy loss to an applied load that is then removed,

unlike pure elastic materials. Relaxation (decrease of stress when subjected to a constant strain) and creep (rearrangement of polymer chain when subjected to stress) are two main characteristics of this kind of materials. About mechanical characteristics such as stiffness, water or ionic liquid solution within the polymer is a key parameter. Stiffness is seen to be increased because of the presence of ions acting as cross-linking agents (Eisenberg and Kim, 1996). When hydrated, the existence of ions also allows the material to have conductive properties (Bautista-Rodríguez et al., 2009) and, therefore, serve as an actuator when coated both faces with electrodes.

Fluoropolymer actuators have been prepared by soaking in water for a period close to an hour at high temperatures and submerging the material after electroding into an acid solution such as sulphonic acid or hydrogen chloride (HCl) (Kim et al., 2011; Franti Opekar and Svozil, 1995; Nguyen, Lee, and Yoo, 2007; Uchida and Taya, 2001; Nouel and Fedkiw, 1998). The H^+ counterions of these acids can be changed for other cations such as lithium (Li) or sodium (Na) just by immersing it into the desired cation hydroxide solution (Bhandari, Lee, and Ahn, 2012). For example, HCl in the presence of a solution of NaOH will change H^+ proton for Na^+, creating a chloride salt (NaCl, sodium chloride). Some others have also tried with directly submerging the material into water when actuating for maintaining the hydration constant (Opekar and Stulik, 1999). When water is present in the membrane water clusters form, and water channels are created among them. Ions are able to move through these channels and to change position due to an electrical stimulus. Which is the basis for actuation.

4. Pre-fabrication and pre-testing preparation

In this chapter the prior characterization of the material is going to be attained. In particular, Differential Scanning Calorimetry (DSC) and Thermo-gravimetric Analysis (TGA) are going to be performed. We are going to use the information taken out of these tests for the latter processing of the material.

4.1. Differential Scanning Calorimetry (DSC)

The differential scanning calorimeter used was a TA Instruments Q2000 equipped with Tzero cell technology and able to heat up to a temperature of 725ºC with high rates of 50ºC/min. More additional information about DSC technique is available in *Appendix II*.

Samples are placed in a capsule and closed hermetically using a press. The reference is another capsule of the same kind but empty. In this case, aluminium capsules were used and mass was measured when samples were prepared. The parameters inserted in the DSC program for the thermal treatment are tabulated in *Table 4*.

Table 4: Values for the parameters needed to specify the thermal treatment to which samples are subjected in DSC

Parameter	Value
Gas	Air
Initial temperature [ºC]	20
Temperature increase gradient [ºC/min]	10
Maximum temperature [ºC]	325
Time at maximum temperature [s]	30
Temperature decrease gradient [ºC/min]	10
Final temperature [ºC]	20
Sample interval [s]	1

Different transitions such as glass transition temperature (T_g), melting or crystallization point can be found using a DSC machine, the most characteristic ones for this study are explained in *Appendix II*.

In *Figure 20* one can see the DSC results for this fluoropolymer in a graph showing Heat Flow (W/g) vs. Temperature (ºC). Exothermic peaks are shown upwards and some data is also specified in the figure.

Melting occurs at 256ºC and the T_g is found at 145ºC . Another endothermic peak can be seen at 170ºC but no explanation has been reached not in the literature nor by using other characterization techniques, although we consider that it may be caused by the evaporation of some solvent.

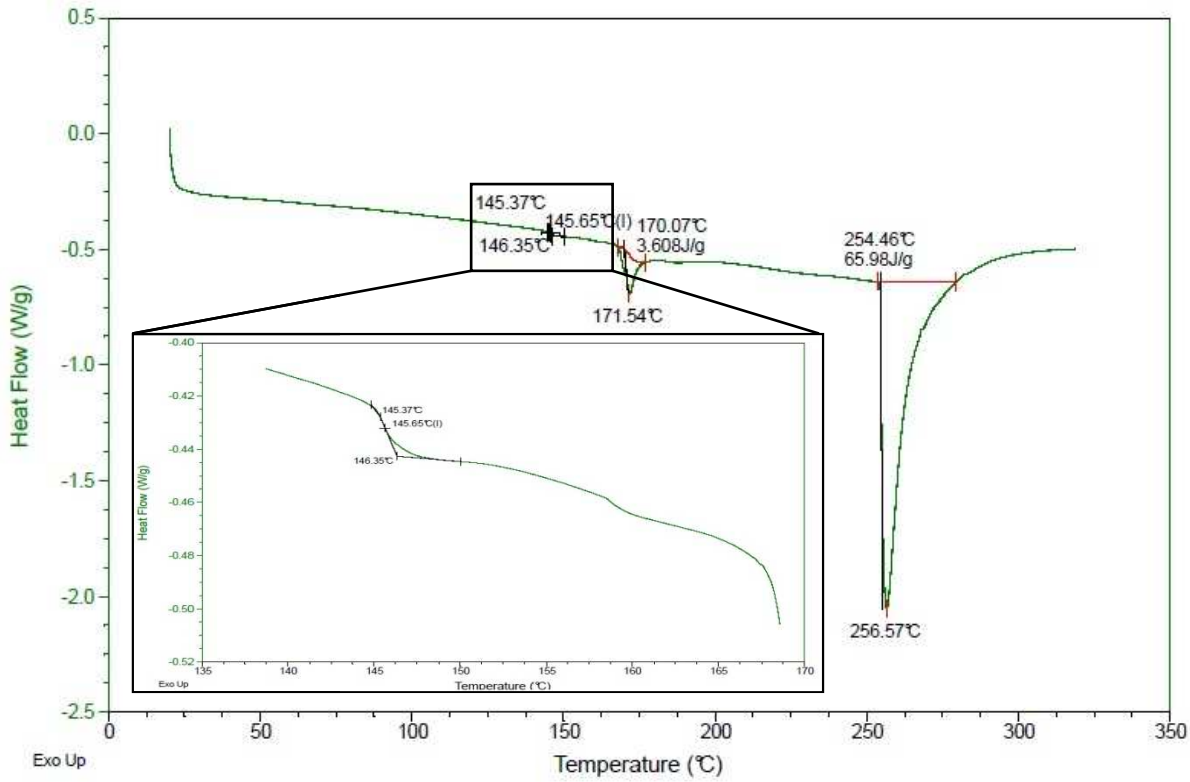

Figure 20: DSC results for the fluoropolymer used as a base for an IPMC actuator. The T_g and the endothermic peak at 170ºC are amplified under the main DSC curve for better observation.

4.2. Thermo-gravimetric Analysis (TGA)

The TGA used was a TA instruments Q50 that is composed by two thermocouples. One of them is placed directly in contact to the sample whereas the other is placed above it. Both thermocouples function at the same time with the same heating rate in order to control the temperature measurements precisely, and the temperature readings serve as feedback to re-adjust the desired temperature. Q50 TGA is equipped with a

horizontal purge gas system that purge gas across the sample and is also able to prevent backflow and minimize buoyancy effects (TA Instruments, 2012b). More information about the TGA technique is available in *Appendix III*.

A 5.5mg sample was prepared and subjected to study in the TGA machine. Parameters that were needed to insert to the program are specified in *Table 5*. From *Figure 21* it is possible to see the percentage of weight varying with temperature. Degradation can be seen to start at around 322ºC and be completed at 500ºC with a 91.3% mass loss. Even though samples were not dried before performing TGA, no significant water content is present in the sample: less than a 0.5% weight decrease is reported from 90 to 110ºC. Furthermore, less than a 0.2% weight variation is seen from 160 to 180ºC, the range where the unexpected endothermic peak of the DSC appeared. No relevant residual mass is obtained at the end of the process.

Parameter	Value
Initial temperature [ºC]	20
Final temperature [ºC]	900
Sample mass [mg]	5.53
Temperature increase rate [ºC/min]	10
Cooling time [min]	20
Sample interval [s]	1
Gas	Air

Table 5: Values for the parameters needed to specify the thermal treatment to which samples are subjected in TGA.

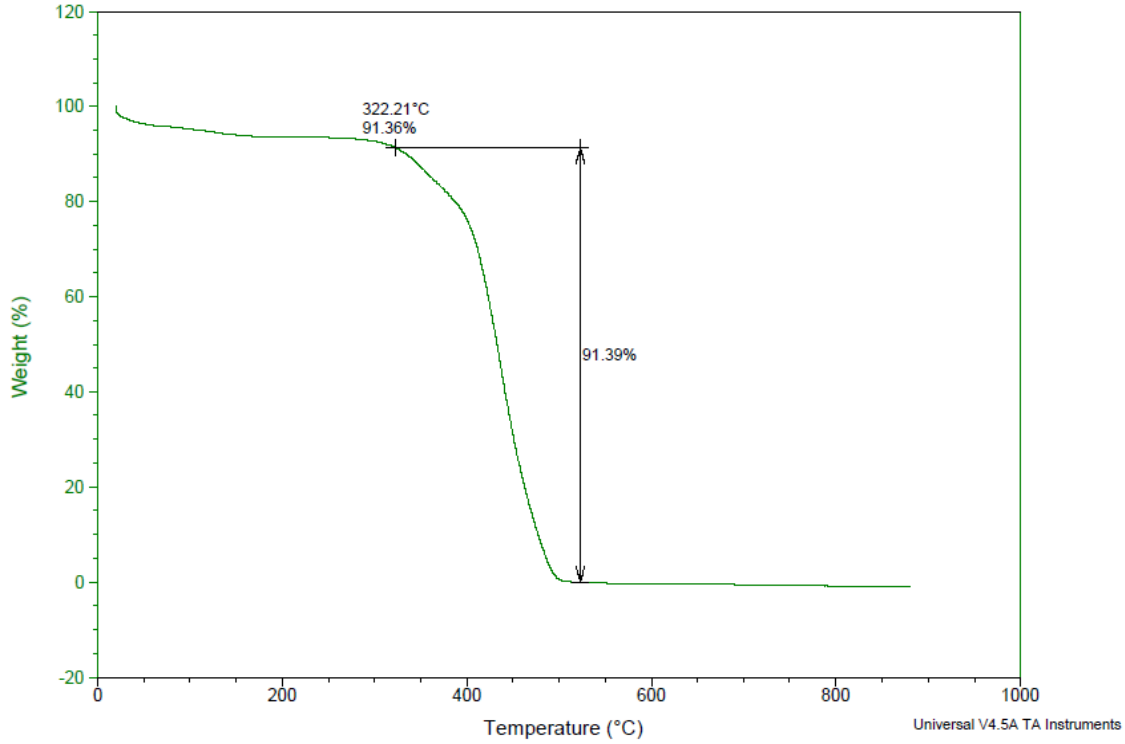

Figure 21: TGA results for the fluoropolymer used as a base for an IPMC actuator.

5. Fabrication of the Ionic Polymer-Metal Composite

This chapter is dedicated to the explanation of the preparation and building process of the IPMC actuator. An IPMC is a sandwich structure composed by a polymeric thin membrane coated in both sides with metallic electrodes.

The membrane is processed using a hot-plate press in order to achieve the require thickness, since a thin membrane (in the micrometer scale) need to be achieved. Gold electrodes are deposited by sputtering on the membrane surfaces.

In contrast to what is explained previously in this document, in this case, the membranes were not soaked in water or submerged in any kind of acid solution to improve its actuation properties. As an alternative, ambient humidity plays a significant role hydrating the membranes. No pre- or post-treatment is performed to hydrate the films or change the counterion present in the membrane, as is reported and mentioned previously in this report to be needed. Rough actuation tests were performed in this manner, and actuation occurred as well. This project is going to take this material and characterize it mechanically, electrically and, of course, study its actuation performance as an IPMC.

Two different fluoropolymer types are studied for building the electrolyte of an IPMC actuator. In the first part of this chapter, a description of this process is provided, followed by the electroding process. IPMCs of about 8-10cm diameter are obtained with this process, from which actuators of about 15x4mm are cut.

5.1. Fabrication and characterization of the EAP

Two different fluoropolymer were tested and prepared for actuation. One of them was already puschased as a film of 50.8μm thick and 100g/m^2 and the other one came in form of pellets of 3x4mm and 1.25g/cc.

With the purpose of easy processing, beads were subjected to a Hot-Press Plate to produce a film.

5.1.1. *Fabrication from fluoropolymer films*

Two processing methods were tried for the fluoropolymer membrane.

1st method: cut a piece directly from the film and coat it with gold electrodes in both surfaces.

2nd method: subject a piece of the material to the heat-treatment schematized in *Figure 22* up to a temperature of 280ºC for 5 minutes in a heating plate followed by a slow rate cooling to room temperature (25ºC). Glass slides were used as support for the membrane not to be in direct contact to the heating plate. In order to avoid adherence of the material to the glass support, Teflon was put in between the material and the glass slides. After the heat treatment, gold electrodes were deposited in both surfaces by sputtering.

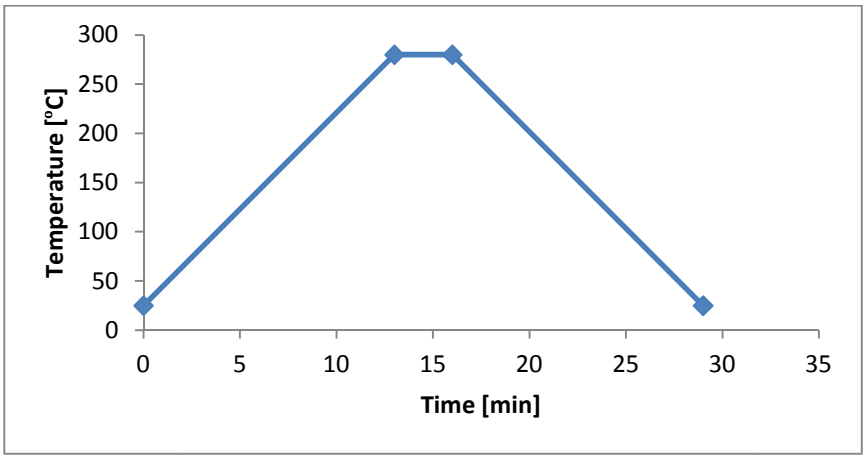

Figure 22: Temperature treatment in heating plate for film specimens. From 25°C room temperature (RT) to 280°C in 11 min (+20°C/min approx.) and back to RT in 11 min (-20°C/min approx.)

Crystallization occurred during the treatment. The brittleness and fragility of the sample when heat-treated are very much increased when compared to the original film. Nonetheless, samples were gold-coated and tried for actuation with negative results.

5.1.2. *Fabrication from fluoropolymer beads*

Several experiments were performed to beads to improve the fabrication procedure and obtain better sample characteristics. Some important parameters were recorded, such as ambient humidity, or controlled, such as maximum temperature, pressure or

temperature rate, in order to optimize the characteristics of the material and its performance against mechanical and electrical tests.

LabPro 400 Hot-Plate press was used to perform the heat-treatment to the material in order to melt the pellets and produce a film, also by the application of pressure. Different lay-ups and temperature treatments were tried and are described in the next paragraphs.

5.1.2.1. Lay-ups for using in hot-plate press

In order that the material did not to stick to the press surface, a low adherence material has to be placed sandwiching the beads. Several set-ups were tried and their advantages and disadvantages are going to be explained in this part of the chapter.

1st lay-up: as *Figure 23-A* depicts, Teflon was used as the low adherence material where pellets are placed. Samples fabricated with this lay-up showed rugosity because of the non-uniform surface of the Teflon sheet used. The drawback of this method is that rugosity may affect stiffness or strength of the manufactured material. However, union among pellets can be successfully achieved.

2nd lay-up: the same concept is used as in the first lay-up structure, also following *Figure 23-A*, but using Kapton instead of Teflon. Kapton sheet surface is much smoother and hence, when subjected to the press, sheets will not show rugosity, as in the previous case. Nevertheless, as can be seen in *Figure 24*, some wrinkles were present in a circular pattern that are thought to be due to some kind of solvent that could not exit the sample set-up once evaporated. Wrinkles still mean surface non-uniformities, which as happens in the previous case, may lead to a decrease in mechanical capacities of the material.

3rd lay-up: metal bands were used in between the press plates to control the resulting membrane thickness. Thickness of the bands depend on the desired thickness of the resulting fluoropolymer sheet. Teflon as also used to sandwich the pellets, as in the first lay-up. *Figure 23-B* shows this lay-up. Metal bands were placed the farthest possible from the beads not to create a thermal gradient within the material that would cause some parts of the membrane to melt faster. Again, Teflon produced surface rugosity in the membrane, as happened for the first case.

4th lay-up: metal bands with a smooth surface were used sandwiching the pellets, as illustrated in *Figure 23-C*. As metal bands are good heat conductors, it was found that the areas of the membrane that were closer to them were slightly degraded, presenting a yellow-brown colour. If temperature was decreased, beads did not fully join.

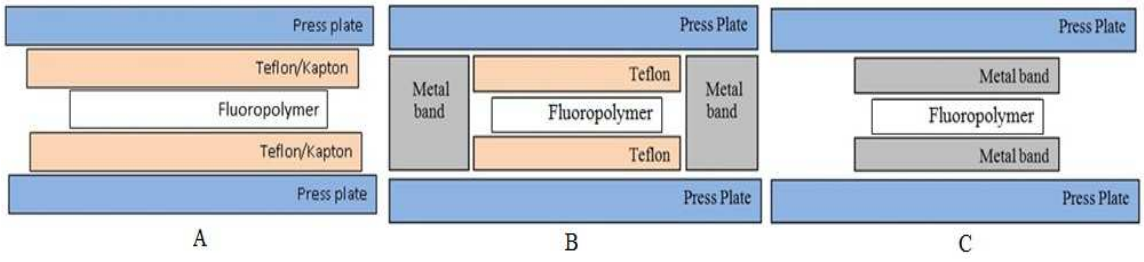

Figure 23: Fabrication lay-ups for fluoropolymer beads to press in LabPro 400 Hot-Plate press.

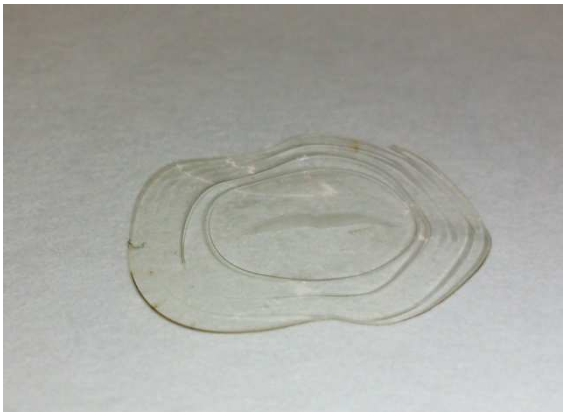

Figure 24: Circular pattern in film processed with Kapton layers. Absence of rugosity may have been provoked for the impossibility to exit of some gas solvent.

Bearing in mind the information about the four different cases above explained, gathered in *Table 6*, it was decided to implement lay-up 3 for the production of films. As the surface would be non-uniform using either Teflon or Kapton, it is preferred to have slight rugosity evenly spattered throughout the whole film than the abrupt surface changes found as wrinkles when Kapton was used. Also, it is important to control the thickness of the film with metal bands rather than just manufacture it getting a random thickness.

Table 6: Comparison of lay-up methods for processing fluoropolymer beads into membranes. In the upper part of the table the different parts of the lay-up are specified ('X' where present). In the lower part of the table observations, advantages and disadvantages are recorded.

Lay-up	1st	2nd	3rd	4th
Teflon for low adherence	X	-	X	-
Kapton for low adherence	-	X	-	-
Metal bands	-	-	X	X
Observations	Rugosity	Wrinkles	Rugosity	Degraded
Advantages	Suitable union among pellets	Smooth surface among wrinkles	Thickness control	Smooth surface
Disadvantages	May affect stiffness or strength No thickness control	May affect stiffness or strength No thickness control	May affect stiffness or strength	Unsuitable union among pellets. May affect material properties

5.1.2.2. Thermal treatment for fabricating the membrane form fluoropolymer beads

Regarding the thermal treatment, several procedures were used to optimize the time of processing and obtaining a membrane suitable for the purpose of this project. Variable factors include maximum temperature, temperature gradients to heat up and cool down the material. In *Table 7* these processes are summarized.

Table 7: Thermal treatments specifications for processing of fluoropolymer beads in a hot-plate press to produce layers.

Thermal treatment	Maximum temperature [ºC]	Temperature rise rate [ºC/min]	Temperature decrease rate [ºC/min]	Observations
1	255	10	-10	Degraded
2	210	10	-10	Fast cooling marks
3	200	10	-10	
4	200	10	-3	Appropriate union among pellets and surface finish
5	190	10	-3	Innadequate union among pellets

The first thermal treatment was designed to reach 255ºC. This temperature profile is shown in *Figure 25*. Samples prepared according to this method showed a slight yellow colour, presumably because of material degradation, as shown in *Figure 26*.

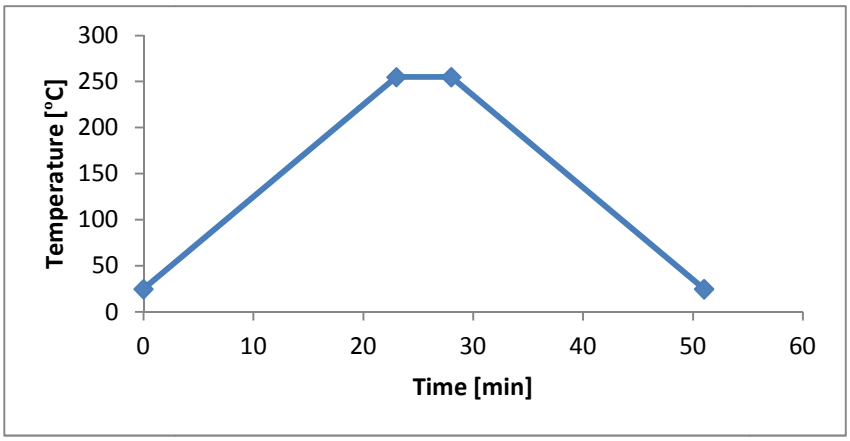

Figure 25: Temperature treatment in press for the two first beads samples from RT up to 255ºC in 23 min (+10ºC/min), stay in 255ºC for 5 min and back to RT in 23 min (-10ºC/min)

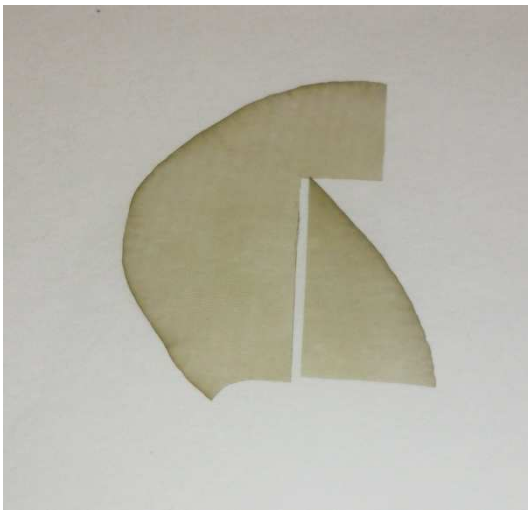

Figure 26:Sample treated at maximum temperature of 255ºC showing yellow colour caused by degradation of the material.

Therefore, 250ºC was set as an upper limit for this treatment. Other possibilities for thermal treatments were set in order to minimize degradation. The lower limit was set by the polymer glass transition temperature, above which the polymer can be shaped. Hence, treatments 2-5 are designed with maximum temperatures from 190 to 210ºC.

While treatment 5 did not give satisfactory results because of deficient adhesion among pellets (190ºC might be too low), treatments 2 and 3 reflect the adverse consequences of fast cooling in the form of marks (see *Figure 27*) that may trigger mechanical characteristics worsening. For this case, other treatments were designed to avoid fast cooling consequences. Treatment 4 present an appropriate maximum temperature and also appropriate temperature increasing and decreasing rates. The temperature profile is shown in *Figure 28*. Correlating this data with the TGA results in *section 4.2.* we can see that there is about a 9% weight that corresponds to the elimination of solvent during the processing of the material.

Figure 27:Sample processed with a cooling rate of -10°/min showing imperfections because of fast cooling,

Pressure at which the material is being subjected during the treatment was also varied when a bigger amount of beads where considered for manufacturing in order to achieve a membrane of the desired thickness. If metal bands were used, as in *Figure 23-B*, the pressure need not to be so much regulated to obtain a particular thickness but it needs to be high enough to layer the pellets to the thickness of the metal shims. Then, the metal bands would prevent the hot-plate press to press further.

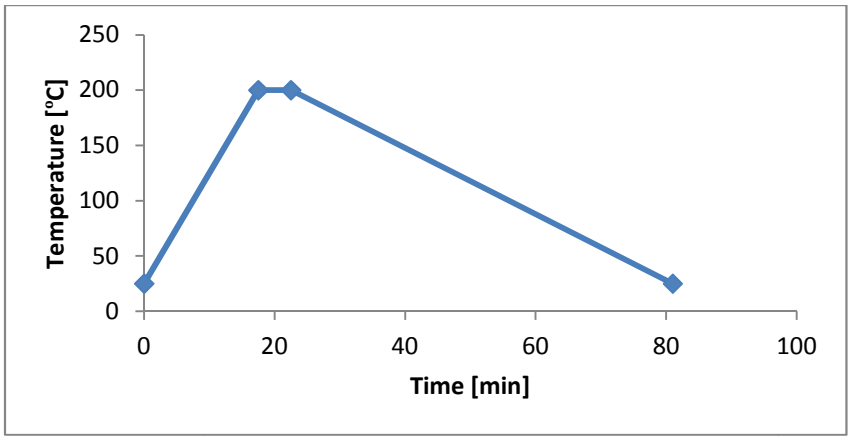

Figure 28: Final temperature treatment in press for beads samples from RT up to the maximum temperature at +10°C/min, stay in the maximum temperature for 5 min and back to RT at -3°/min

After collecting and analysing the results for the five different heat treatments and implementing them with the third lay-up using metal bands as blocking structures for the hot-plate press, the fourth heat treatment using a pressure of 25kN showed to give the best results in terms of absence of degradation, absence of flaws because of abrupt temperature changes, joining of pellets and thickness control. These parameters are consequently going to be used from here on when producing layers.

Tensile test in an INSTRON machine and Scanning Electron Microscopy (SEM) were performed to characterize the EAP.

5.1.3. Mechanical characterization of the EAP

In *Figure 29* and *Table 8* specimens measures are specified. They were cut out of a membrane sheet prepared as aforementioned and prepared for the tensile test attaching cardboard tabs in both ends with a cyanoacrylate adhesive. As it was desired not only to document the stress-strain curve and the elastic modulus of the material but also the way it deformed when subjected to tension, VIC-2D digital image correlation measurement system was used. Movement within the 2D plane is possible to be determined and strains from 50 to over 2000. The sample preparation for this process consisted on painting the specimens' surfaces in white and then speckle them in black so a great contrast between both colours is achieved.

Figure 29:Sketch of an specimen used for tensile test in an INSTRON machine. In white the fluoropolymer, in blue the cardboard tabs and black speckles all over the surface to perform 2D digital image correlation

Table 8: Dimensions for fluoropolymer specimens subjected to tensile test in an INSTRON machine at 1mm/min strain rate.

Dimension	[mm]
Total length	63.5 ± 5
Gage length	23.0 ± 5
Width	3.18 ± 0.03
Thickness	0.21 ± 0.04

The next step was to set the samples in the INSTRON machine and set the VIC measuring system appropriately focusing in the desired area and proceed with the tensile test. The strain rate was set to 1 mm/min and the VIC measuring system was set to take a photo every second during the tensile test.

Results for the tensile tests are a set of values of time, specimen extension, loading, tensile strain and tensile stress. Thanks to these values, the stress-strain curve can be obtained and Young's modulus can be calculated to be around 180MPa at the linear

region of the curve, i.e. strains from 0.07230 to 0.08480. In *Table 9* it is also shown the average results for maximum load applied to the specimens, maximum stress and maximum strain, together with a stress-strain curve example in *Figure 30*. The actual values for each specimen can be seen in *Appendix IV* together with the stress-strain curves.

Table 9: Average of the results from the INSTRON tensile test performed to 8 specimens.

	Value
Maximum load applied [N]	9.9 ± 0.8
Maximum stress [MPa]	17.1 ± 1.4
Maximum strain [mm/mm]	0.39 ± 0.12
Young's modulus [MPa]	180 ± 45

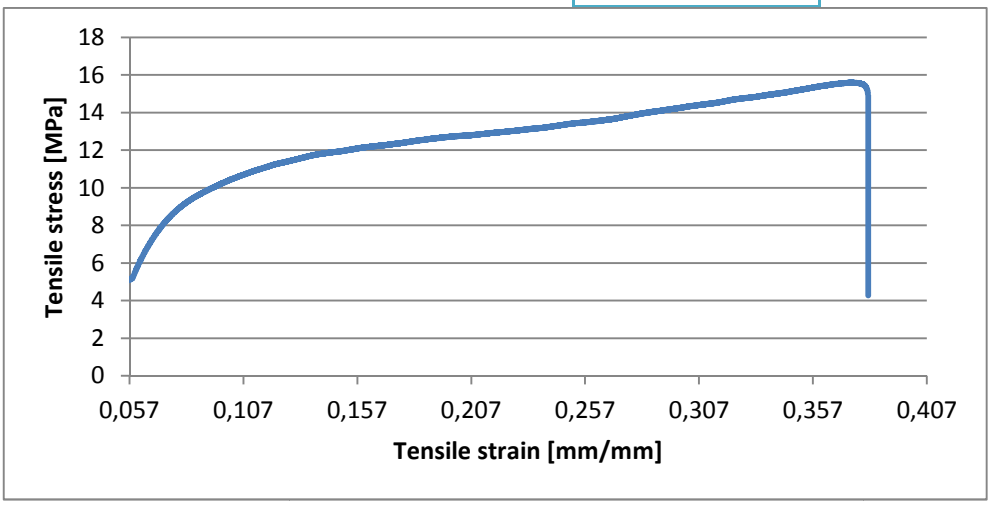

Figure 30: Example of a stress-strain curve for one of the specimens tested under tension in an INSTRON machine, without accounting for the prior adjustments of the equipment.

VIC equipment shows results of deformation within the layer by correlating images. In this way, we can see the areas with higher degree of deformation in the polymer. An example of this can be seen in *Figure 31*.

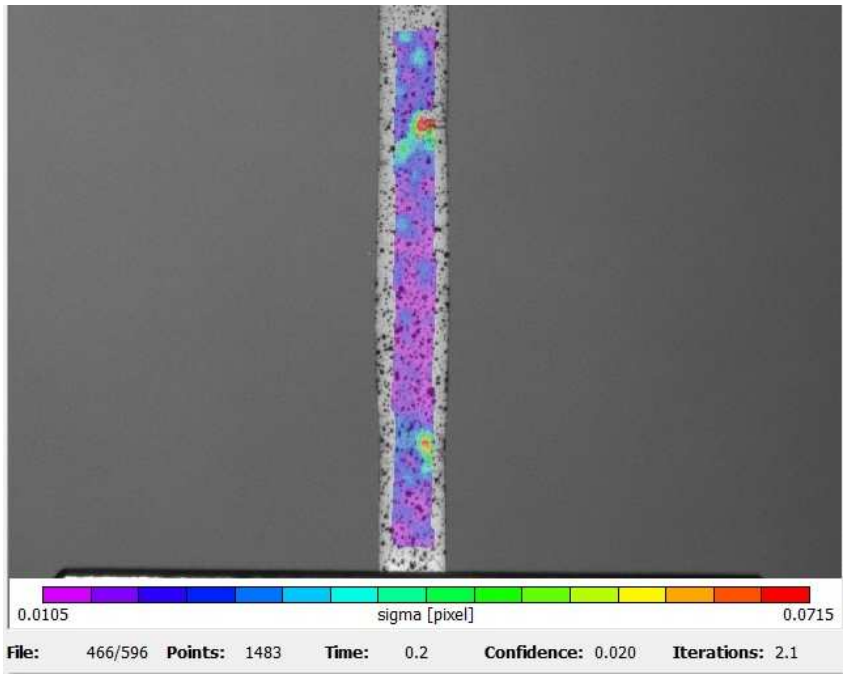

Figure 31: 2D-VIC digital image correlation results on the deformation of the EAP subjected to tension in a INSTRON machine.

5.1.4. Scanning Electron Microscope (SEM) characterization of the EAP

A Zeiss Evo MA15 SEM has been used for morphology analysis of the fluoropolymer membranes as well as for the chemical composition of the samples. It is equipped with chemical microanalysis EDS Oxford INCA350. More general information about SEM is available in *Appendix V*.

Several different samples of about 25mm^2 were prepared and covered with a ~60nm chromium layer by sputtering. Information about the samples is arranged in *Table 10*.

Table 10: Samples of EAP prepared for SEM. Four samples with different characteristics were prepared and tested. Every sample was coated with Cr to obtain SEM images.

Sample	Characteristics
1.1	Normal, plain EAP sample
1.2	Burnt EAP sample for high temperature processing in hot-plate press
1.3	EAP sample tested in tension until failure
1.4	Normal, plain EAP sample, cross-section image

By SEM images one could only observe some tears in sample 1.3 because of the tensile test (see *Figure 32)*. These results contrast with the smooth surface of samples 1.1 and 1.2 (*Figure 33*).

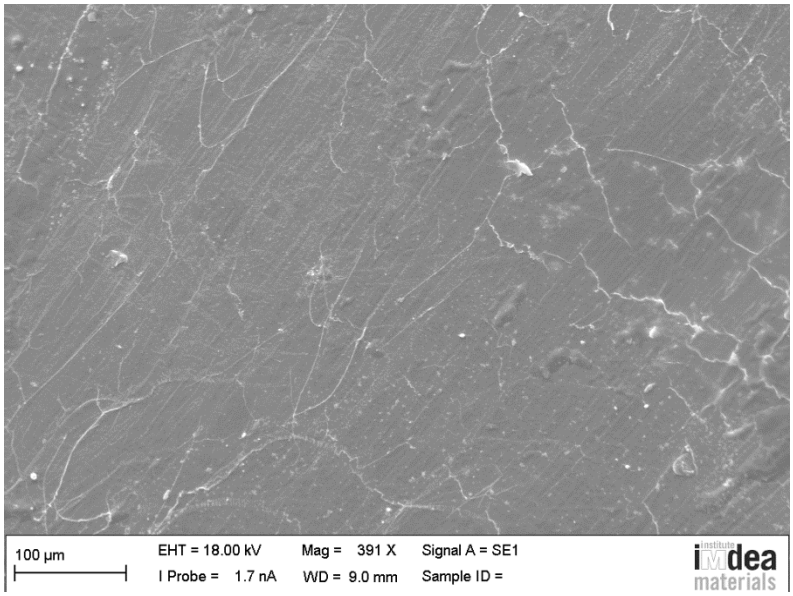

Figure 32:SEM image for sample 1.3 showing tears in the sample as a result of a tensile test performed to the material prior to SEM.

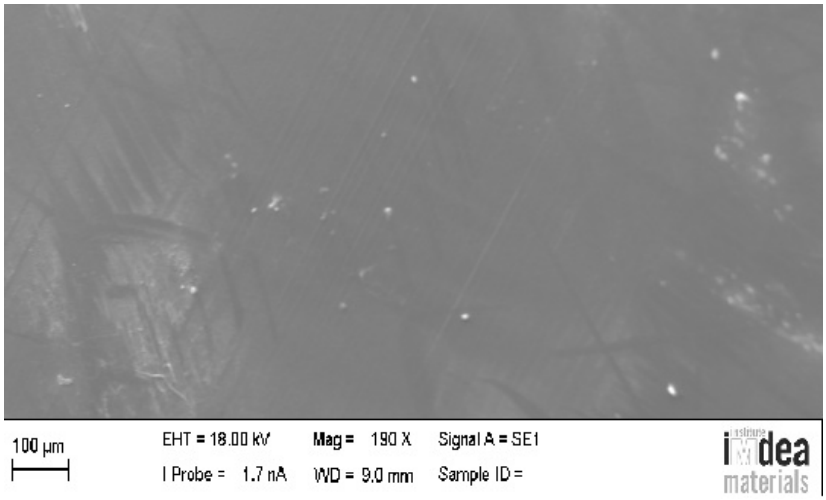

Figure 33: SEM image for sample 1.1. It shows a smooth surface.

Samples 1.4 was thought to study the thickness of the membranes once processed. The aim was to observe any porosity. *Figure 34* show these results, although no porosity can be distinguished in the membranes.

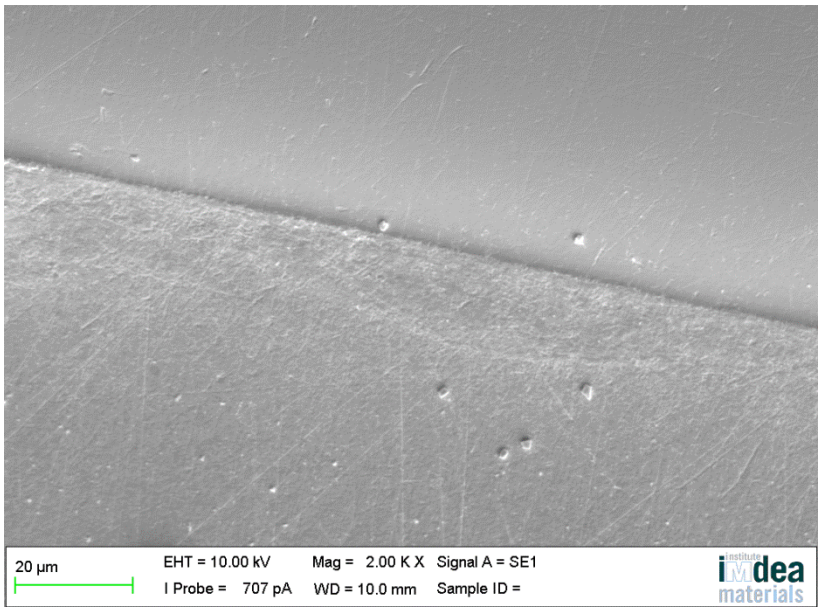

Figure 34: SEM image for sample 1.4 showing the fluoropolymer membrane thickness in a cross-sectional view. No porosity can be distinguished.

5.2. Fabrication and characterization of the Ionic Polymer-Metal Composite

Gold was deposited in the surfaces of EAP films and tried for actuation. Other electrode materials were thought such as carbon nanotubes because of previous studies in ionic actuators (Liu et al., 2010).

5.2.1. Gold deposited electrode

An appropriate electrode needs to be chosen. As reported previously in the literature, noble metals are preferred for their excellent conductivity. Also, one has to bear in mind that an electrode presenting excessive stiffness will not allow a proper motion of the actuator and as a consequence, a thin electrode is required. In this case, gold was chosen as the noble metal and the electroding procedure was sputtering, a physical vapour deposition technique. This method enables a fast and simple way of coating the samples. Thickness of the electrode layer can be also easily controlled by establishing specific parameters of current intensity and time of deposition.

By using the Q150T Turbo-Pumped Sputter Coater, gold is deposited in both faces of the membranes, as can be seen in *Figure 35*. It can be seen the roughness of the material once covered with the Au electrode. The parameters used for current and time of deposition are shown in *Table 11*. However, the sputtering was not very effective adhered so it can be removed easily by touching or scratching it.

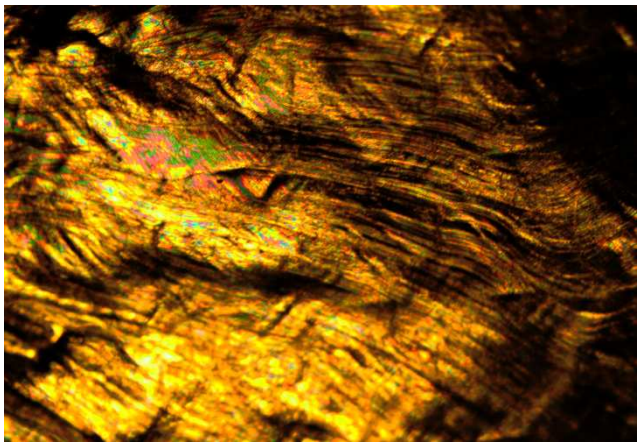

Figure 35: x50 Optical microscope image of a gold covered fluoropolymer membrane.

Table 11: Parameters for Au sputtering

Current [mA]	Time [s]	Au layer thickness [nm]
60	30	30 (on each face)
40	120	70 (on each face)

In the first experiments for actuation it was shown that the second case, with 40mA during 120s was more effective than the first one. Actuation became visible with lower voltage (perhaps because some of the Au sputtering was already gone in the samples with the first coating) but a thicker Au layer was proved to be better for actuation, so the second case was used for the rest of Au deposited electrode samples.

Characterization of the IPMC is performed by SEM.

5.2.2. Scanning Electron Microscope (SEM) characterization of the IPMC

The same Zeiss Evo MA15 SEM has been used in this case for the characterization of the IPMC. Samples were of the same size again, i.e. 25mm^2. In *Table 12* some information is available about the samples.

Table 12: Samples of IPMC prepared for SEM. Three samples with different characteristics were prepared and tested.

Sample	Characteristics
2.1	Normal, plain IPMC sample
2.2	Sample of IPMC tested in actuation for fatigue failure
2.3	Normal, plain IPMC sample, cross-section image

In sample 2.2 (*Figure 36*), in contrast to the smooth surface of sample 1.1, there are some lines that are possibly due to the loss of Au electrode during the 23h of continuous actuation.

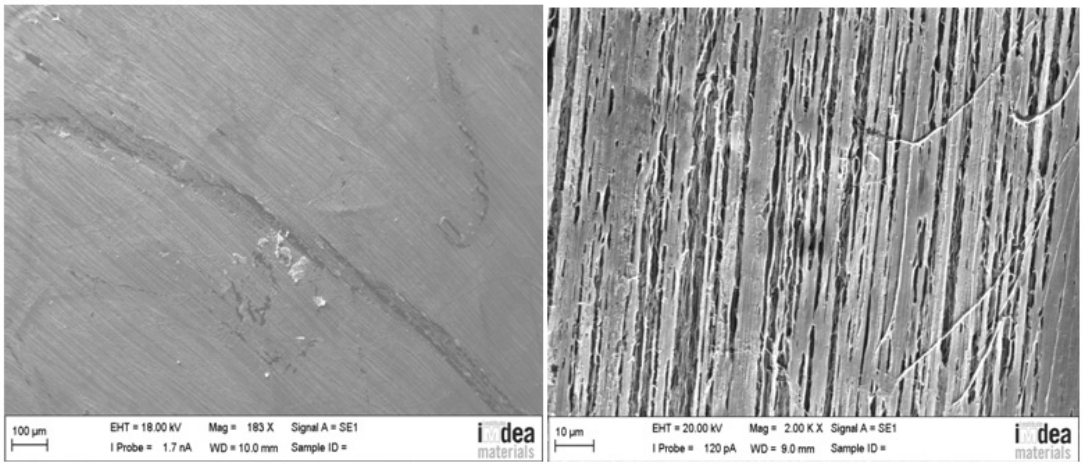

Figure 36: SEM image for sample 5 showing the anisotropy of actuation at 100 (on the left) and 10µm (on the right). It is possible to see parallel longitudinal flaws that were provoked by the uninterrupted actuation during 23h most likely for the loss or consumption of the Au electrode.

Sample 2.3, in *Figure 37*, was intended to study the cross-section of the IPMC membranes and the gold layer surrounding the EAP. Once more, there is no observable porosity, yet the thin gold later deposited by sputtering is visible.

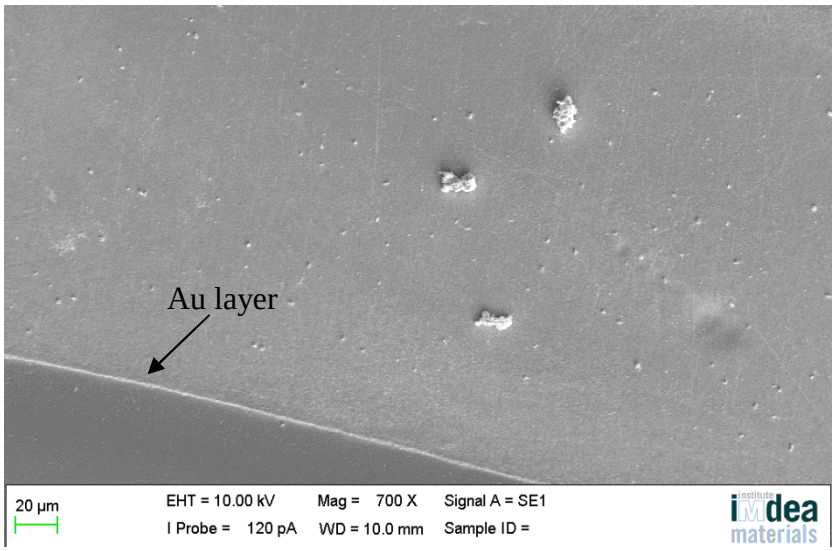

Figure 37: SEM image for sample 7. It is possible to distinguish between the fluoropolymer membrane and a thin gold layer covering it.

The chemical composition was also studied in case some explanation for the peak at 170ºC in DSC was reached. However, the components of the sample were always the expected ones: fluoride, a very small amount of sulphur (~4%), gold in the cases where the electrode was already deposited and chromium for the sputtering in order that better electron conductivity was obtained. An example of this report for results of sample 5 is shown below in *Figure 38*.

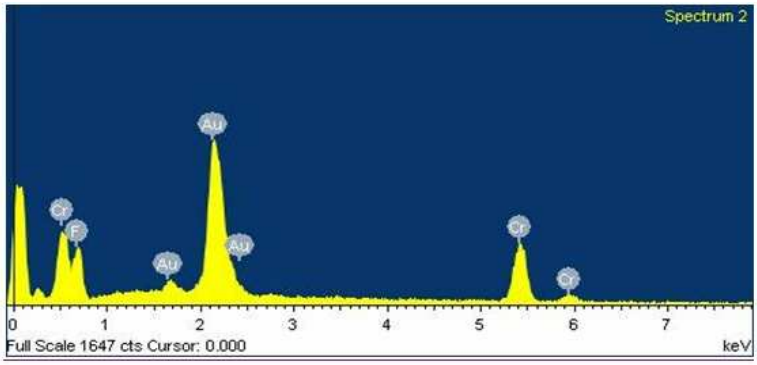

Element	Weight%	Atomic%
F K	37.86	77.69
Cr K	18.13	13.59
Au M	44.01	8.71
Totals	100.00	

Figure 38: BSE analysis in SEM for sample 5 of the fluoropolymer subjected to fatigue in actuation during 23h. Chemical components are shown in weight and atomic percentage.

6. The actuation mechanism of the IPMC

Different studies were performed to investigate the actuation mechanism of the fluoropolymer membranes. In this chapter the working bench and the set-up for this experiments are described followed by several subchapters where the experimental studies carried out on actuation of the membranes are presented.

6.1. Set-up for actuation:

The working bench is formed by a telemetric laser, a data acquisition card, a function generator and a computer in charge of data collection and processing (*Figure 39 and 40*).

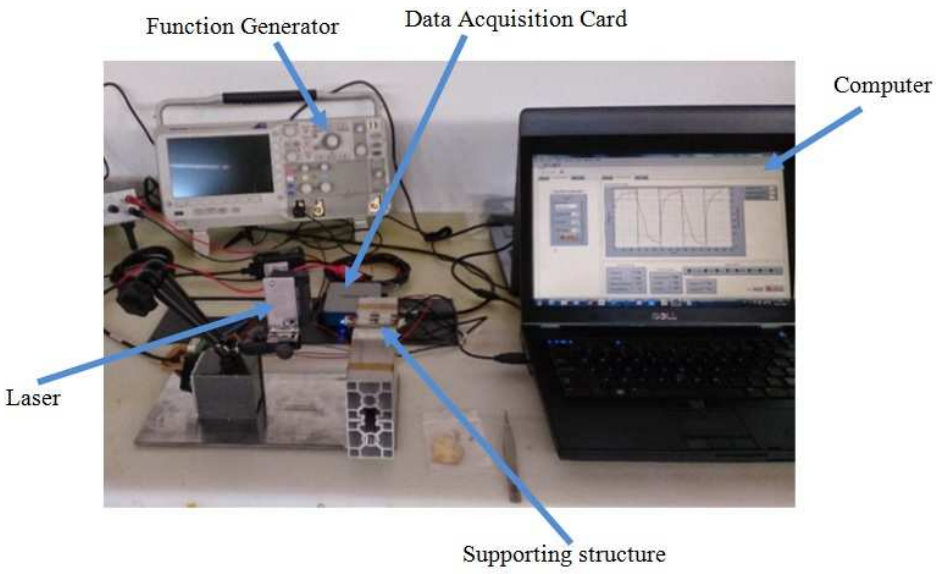

Figure 39: Working bench formed by a telemetric laser, data acquisition card, function generator and the computer

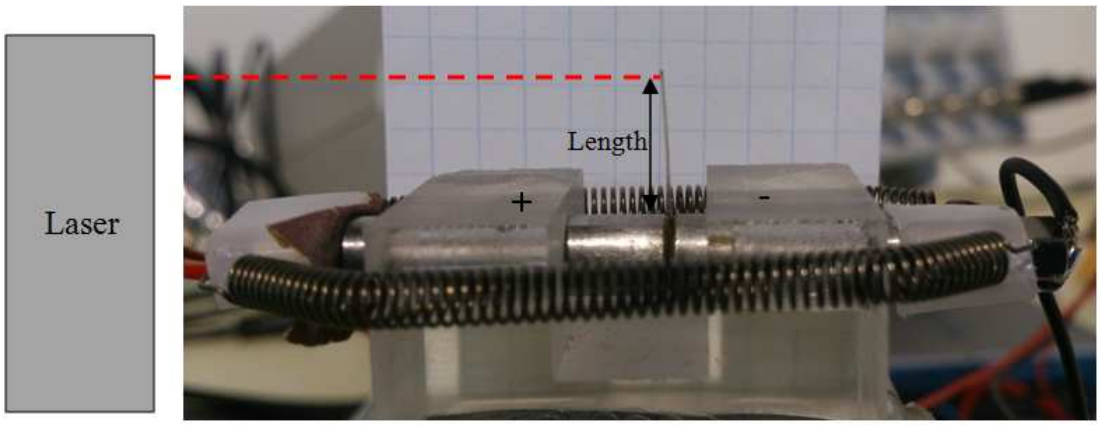

Figure 40: Supporting structure for the IPMC actuator.

The function generator (Aim&Thurlby Thandar Instruments TG550) is in charge of applying an electric field to the material so that it bends as part of its actuation mechanism. The reason why a function generator is required is because, to perform the full study, it is required to be able to supply negative and positive electric fields. With a function generator is therefore possible to choose the frequency, voltage amplitude and the type of wave supplied. The function generator was connected to the material via a holding platform.

The telemetric laser used in this experiment (IL series, from Keyence) has an accurate resolution of ±0.01mm when measuring the distance to an object within 5cm distance. Since the laser is directed to the tip of the actuator, it can measure the maximum deflection of the membrane, as it mounted in a cantilever configuration. The laser is connected to the computer by a data acquisition card. With the data acquired from it, a precise actuation characterization is possible to be performed.

The data acquisition card is in charge of collecting and transferring data from the telemetric laser to the computer. The one used for this experiment is a USB NI-6002 National Instruments card with LabVIEW software,

The computer is equipped with a software that enables the user to manage the data acquired from the laser. Once the program is set initiated and the record function is active, a graph is being created at the same time as the data is being collected. The resulting graph express the displacement measured by the laser in millimetres versus

time. Graph and data can be exported to an Excel file for later studies (Rubalcaba Sánchez, 2015).

6.2. *Studies on actuation of IPMC:*

Several studies were performed to characterize the fluoropolymer membrane as an actuator. In *Figure 41* one can see an example of input and output of actuation. A square wave voltage is applied to the IPMC electrodes and bending occurs, which is indeed measured at the specimens tip. Even though the input electric signal is squared, the output tip displacement behaves differently.

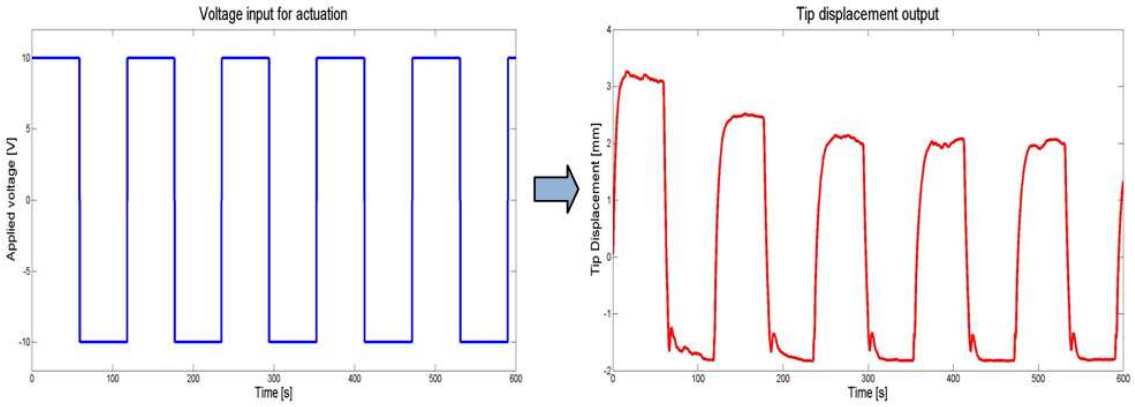

Figure 41: Example of input and output for actuation of the IPMC specimens.

It was subjected to a constant electric field and to periodic signals. As far as periodic signals are concerned, comparative studies were carried out varying the voltage (signal amplitude) or the frequency of the wave. On the other hand, the geometry of the IPMC was also varied. In the following table (*Table 13*) a summary of the studies is provided and in *Table 14* more detailed information is given regarding the tests to be performed. Results are going to be attended in subsequent parts of this chapter.

Table 13: Main objectives and aims to perform each study on a IPMC actuator.

Study:	Objective:
Constant electric supply	See the actuation behaviour over a long period of time under a constant voltage. Quantify the bending deformation of the material as a response to a certain voltage and see if it suffers bending relaxation.
Periodic signal electric supply	See the dependence of actuation on the amplitude and frequency of the signal. Study the point for each voltage at which the maximum deformation is achieved.
Geometry variation	See the dependence of actuation on the length, width and thickness of the membrane.

Table 14: Studies performed for actuation of fluoropolymer membranes coated with gold electrodes. Three thicknesses are going to be studied and are placed in the columns of the table. The different tests are named below and the ticks correspond to the tests that were performed.

Thickness [mm]	0.09	0.17	0.22
Voltage Scan	✓	✓	✓
Frequency Scan	✓	✓	✓
Length variation	✓		
Fatigue	✓	✓	✓
Long time exposure	✓	✓	✓

6.2.1. Voltage scan

For voltage scan one sample of each thickness was used trying to cut them with similar width and length. Voltage was varied 1V at a time to each electrode, which makes it 2V amplitude variation when talking about a periodic signal. The final voltage is set to be 10V (20V amplitude). The parameters in *Table 15* were set for every sample under this study. The detailed procedure followed to perform this study can be seen in *Appendix VI*.

Table 15: Actuation parameters to study the behaviour of the IPMC actuator for different voltages (2-20V peak to peak).

Parameters	0.09mm	0.17mm	0.22mm
Type of wave	Square wave		
Frequency [Hz]	0.008		
Data acquisition interval [s]	0.1		
Number of cycles to record	5		
Time between tests [min]	2		
Relative humidity [%]	32	22	36
Sample size [mm^3]	10x3.92x0.09	10x3.91x0.17	10x3.96x0.22

Data is collected in Excel sheets and loaded to Matlab to be processed. Two graphs are obtained, the first showing tip deformation versus time and the second one showing tip deflection amplitude (maximum distance between deflection to anode and cathode) per cycle. In the following figures (*Figure 42-47*) results can be seen for all the three thicknesses for even values of voltage. Graphs with voltages from 1V to 10V are available in *Appendix VII*.

a) Membrane thickness of 0.09mm:

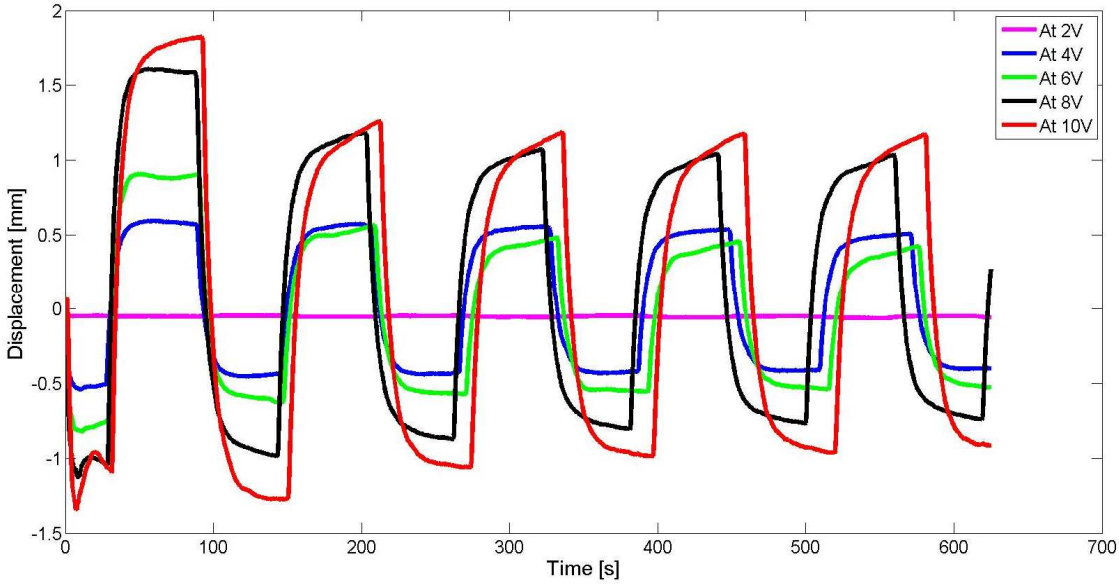

Figure 42: Graph representing displacement of the actuator tip in millimetres versus the time of actuation for an actuator of 0.09mm of thickness. Each line is representing a different voltage.

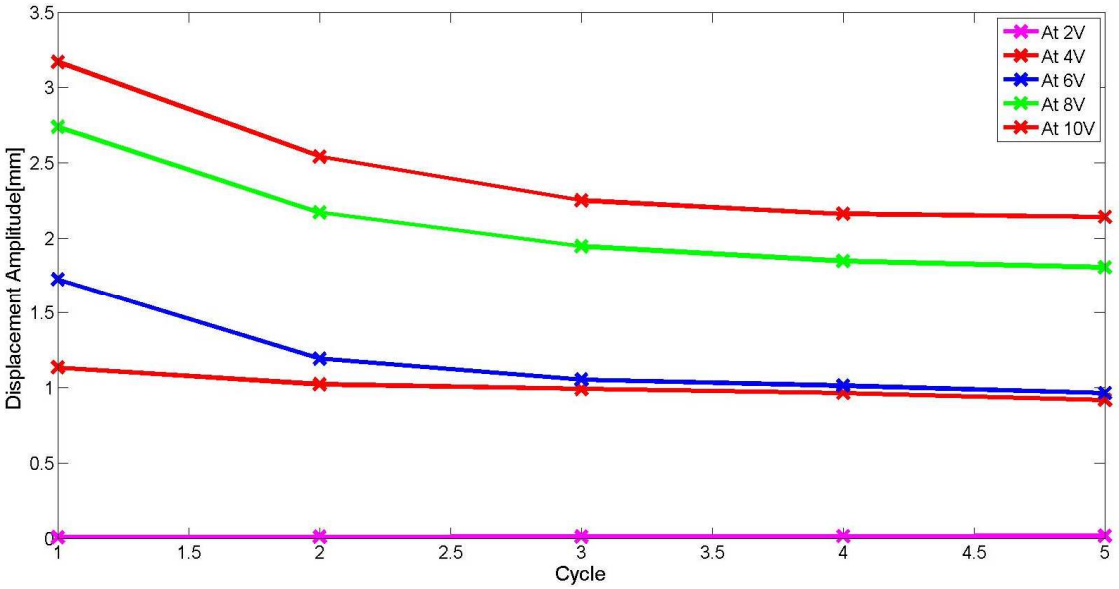

Figure 43: Graph representing the displacement amplitude for an actuator of 0.09mm of thickness versus cycles of actuation. Each line is representing a different voltage.

In *Figure 42* the actual displacement of the tip of the actuator can be seen subjected to various voltages. It can be appreciated that the displacement is not centred in 0mm but shifted upwards in the graph, which means that the actuator does not evenly move towards each side. To study the displacement amplitude, that is, the distance from the maximum deflection in both directions, *Figure 43* is built.

According to these two last figures, the higher the voltage supply, the wider the tip displacement. Also, according to *Figure 42*, actuation at 6V appears to be lower than it should.

b) Membrane thickness of 0.17mm:

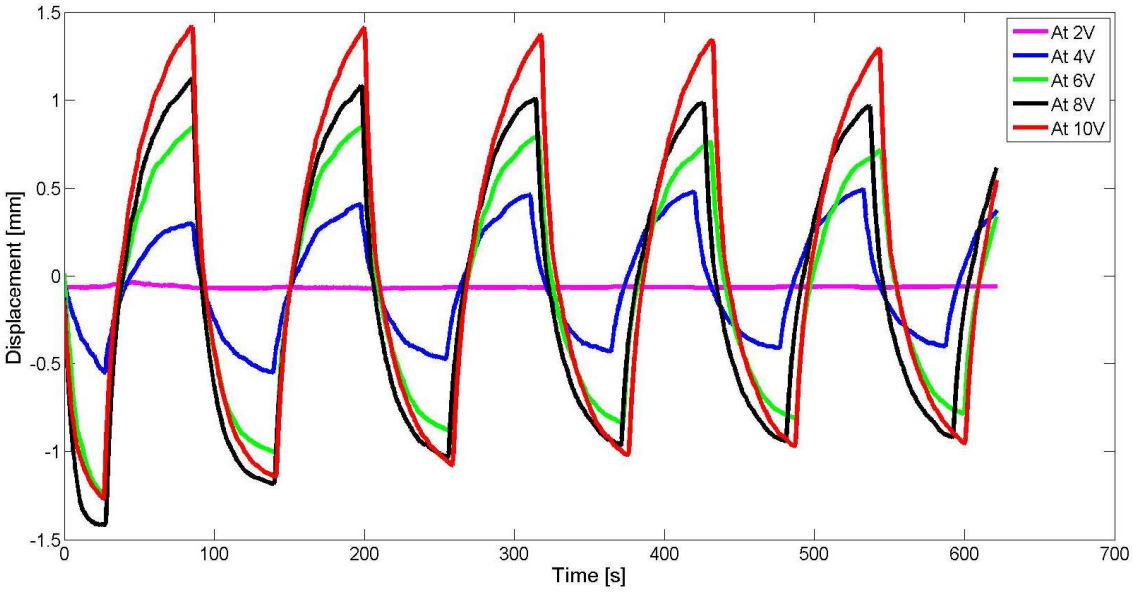

Figure 44: Graph representing displacement of the actuator tip in millimetres versus the time of actuation for an actuator of 0.17mm of thickness. Each line is representing a different voltage.

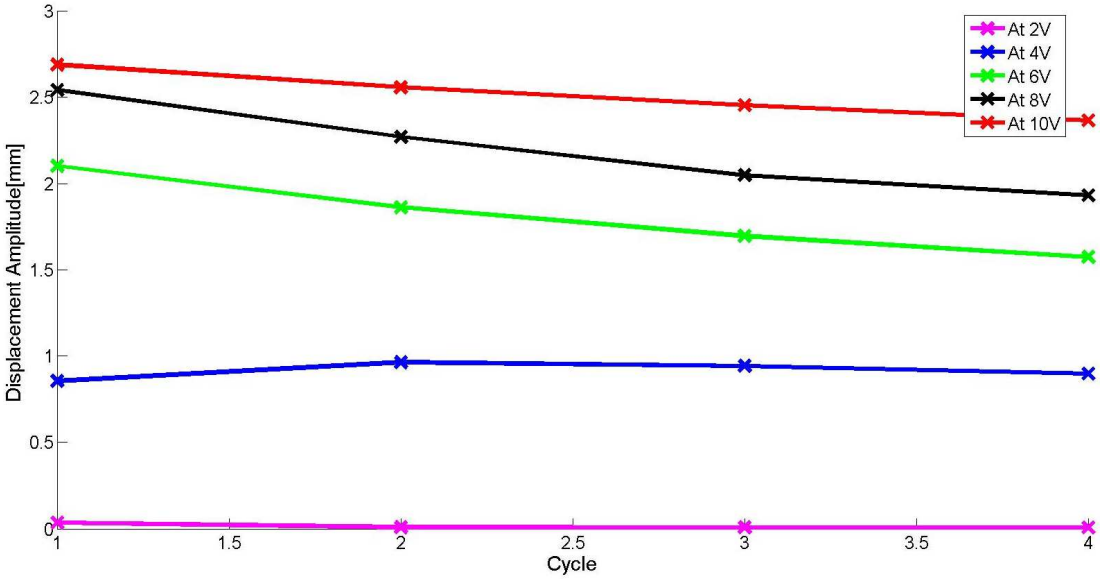

Figure 45: Graph representing the displacement amplitude for an actuator of 0.17mm of thickness versus cycles of actuation. Each line is representing a different voltage.

As for 0.09mm thickness specimens, the actuation results are coherent.

c) Membrane thickness of 0.22mm:

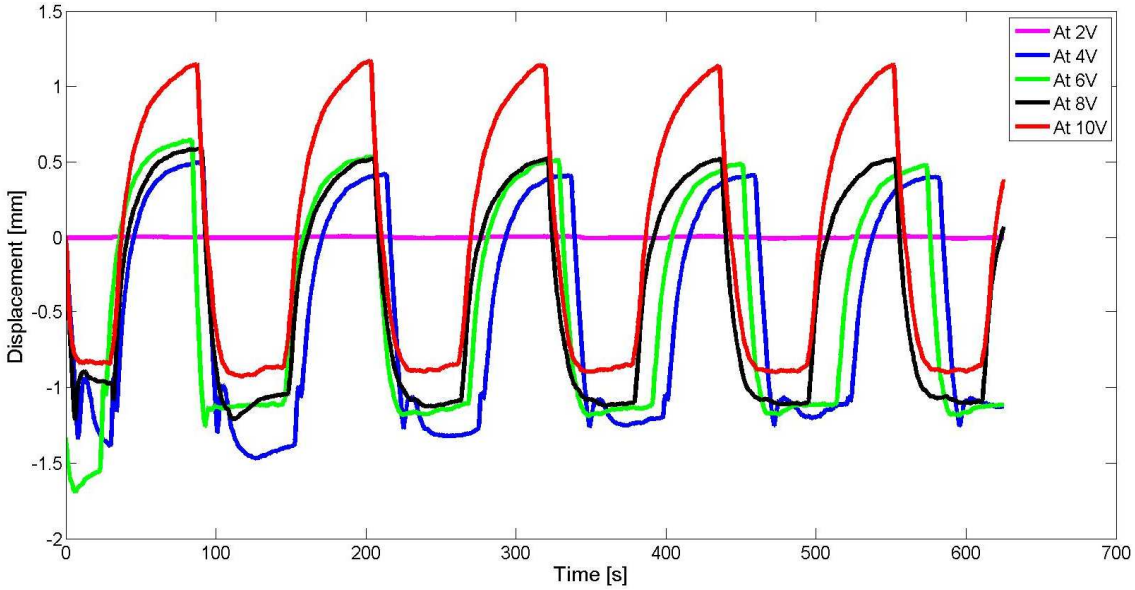

Figure 46: Graph representing displacement of the actuator tip in millimetres versus the time of actuation for an actuator of 0.22mm of thickness. Each line is representing a different voltage.

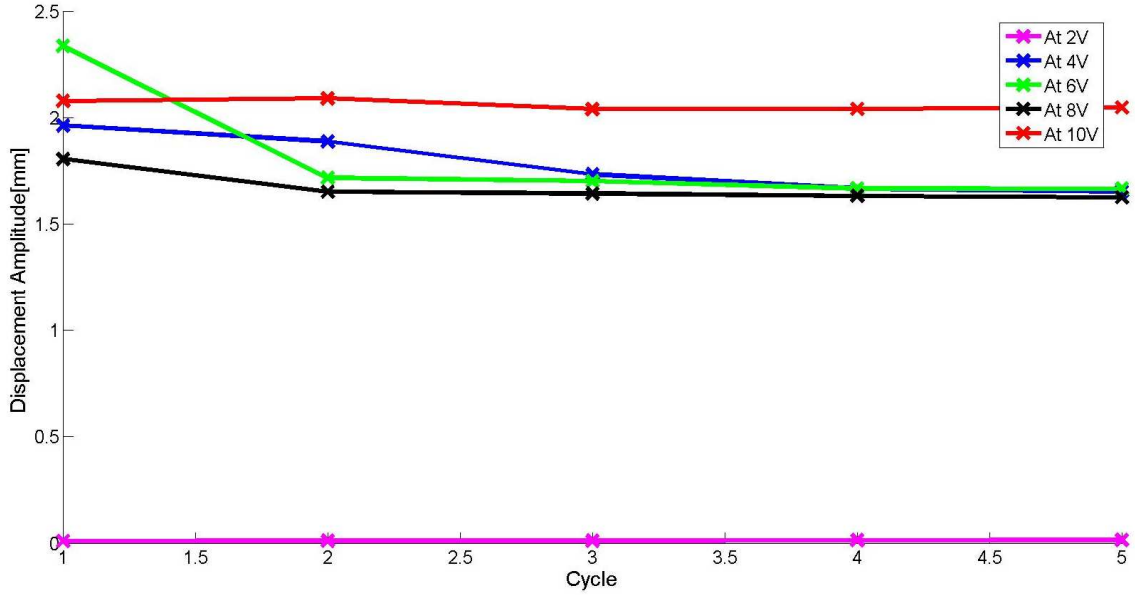

Figure 47: Graph representing the displacement amplitude for an actuator of 0.22mm of thickness versus cycles of actuation. Each line is representing a different voltage

The fact that some results appear illogically scattered from the rest cannot be yet explained. Relative humidity when processing the samples and when actuating could become relevant, but the percentage of variation was negligible within samples of the same thickness.

For a better analysis of these results, comparative graphs have been also obtained. Data is compiled and showed for tip displacements of the three thicknesses for two sample voltages of 4 and 8V. This graph can be seen in *Figure 48*. Again, contrary to what was expected, the 0.09mm thickness specimens were not the ones experimenting higher deflections but so were the 0.17mm thickness specimens.

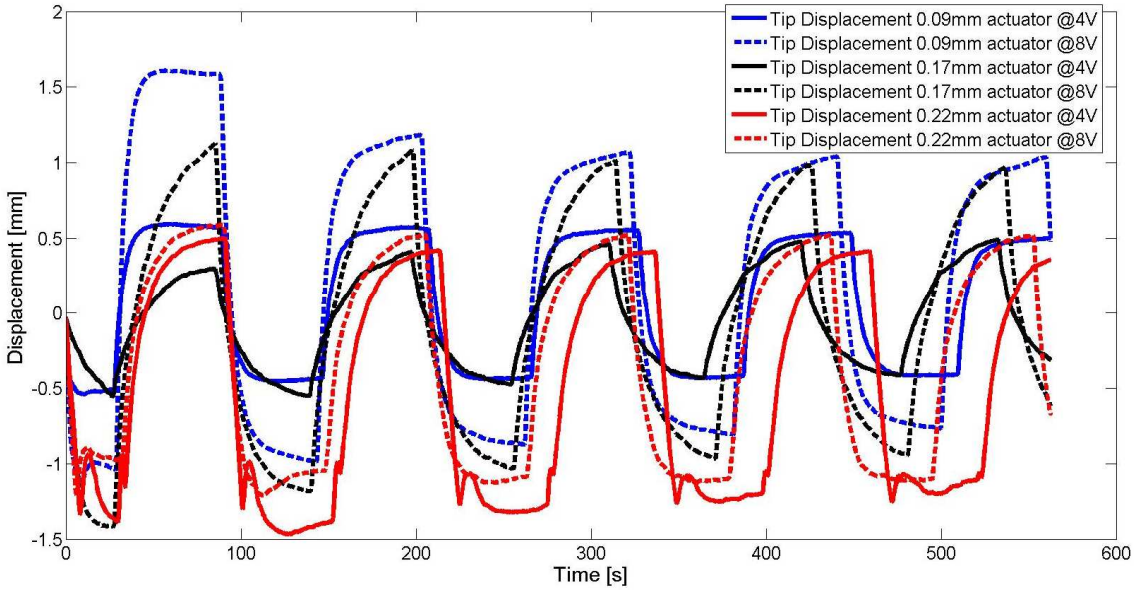

Figure 48: Graph showing displacement versus actuation time comparing three different thicknesses (0.09, 0.17 and 0.22mm) at two different voltages (5 and 10V).

6.2.2. Frequency scan

For frequency scan one sample of each thickness was used trying to cut them with similar width and length. Frequency of the electric signal was varied (1-500mHz), keeping the voltage set to 5V (10V tip to tip). The parameters in *Table 16* were set for every sample under this study.

Table 16: Actuation parameters to study the behaviour of the IPMC actuator for different frequencies (1-500mHz).

Parameters	0.09mm	0.22mm
Type of wave	Square wave	
Voltage [V]	5	
Data acquisition interval [s]	0.1	
Number of cycles to record	2-5	
Time between tests [min]	2	
Relative humidity [%]	31	30
Sample size [mm]	10x4.04x0.09	10x3.96x0.22

Data is again collected in Excel sheets and processed in Matlab. The obtained graphs show tip deformation versus time for each frequency and the second one showing tip deflection amplitude (maximum distance between deflection to anode and cathode) at each frequency. The detail procedure of these tests can be read in *Appendix VIII*. In the following figures (*Figure 49-52*) results can be seen for 0.09 and 0.22mm thickness specimens for two values of frequency i.e. 5 and 100mHz. For the rest of the values for frequency, graphs in *Appendix IX* can be consulted.

a) Membrane thickness of 0.09mm:

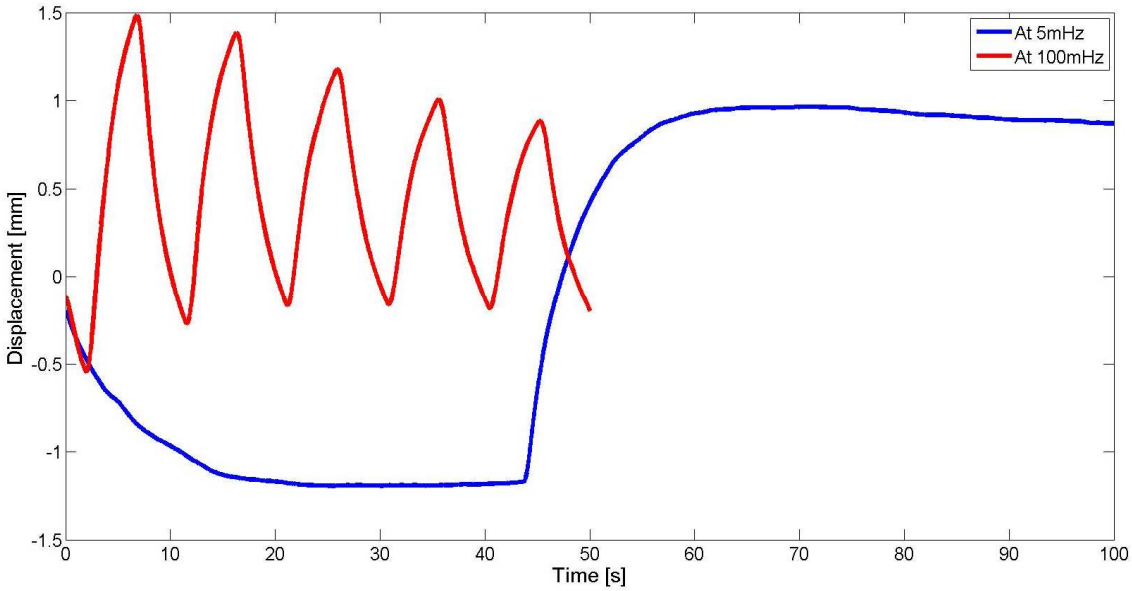

Figure 49: Graph representing displacement of the actuator tip in millimetres versus the time of actuation for an actuator of 0.09mm of thickness. Each line is representing a different frequency. Only five cycles are shown for actuation at 100mHz.

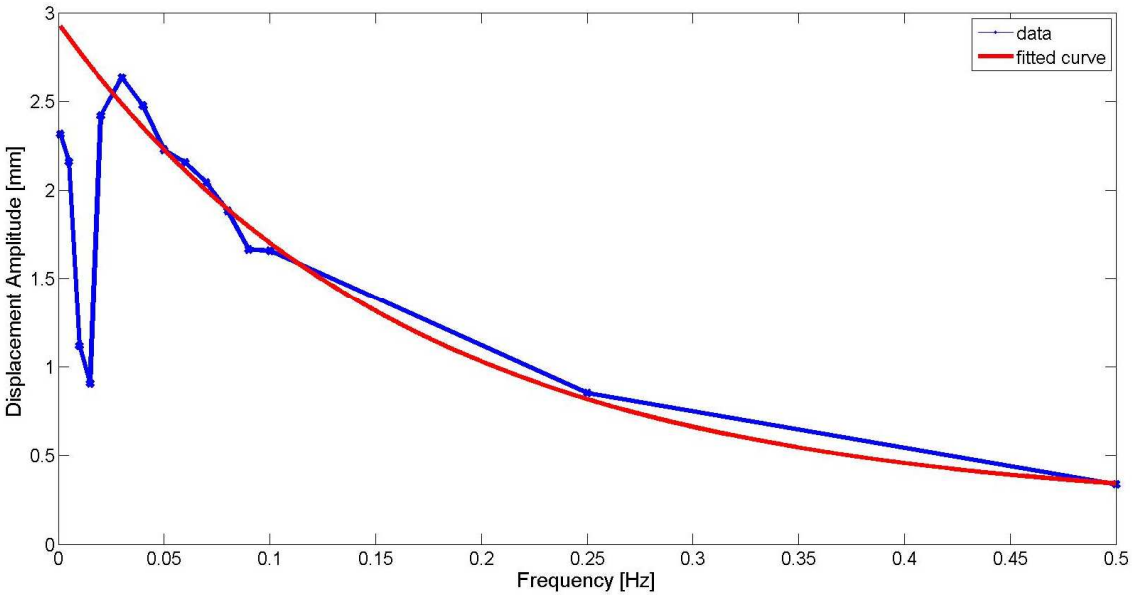

Figure 50: Tip deflection amplitude for an actuator of 0.09mm thickness. Actual data can be seen in the blue curve. The red curve is a fitted curve of the values from 0.02 to 0.5mHz (values from 0.001 to 0.015mHz have been ignored).

b) Membrane thickness of 0.22mm:

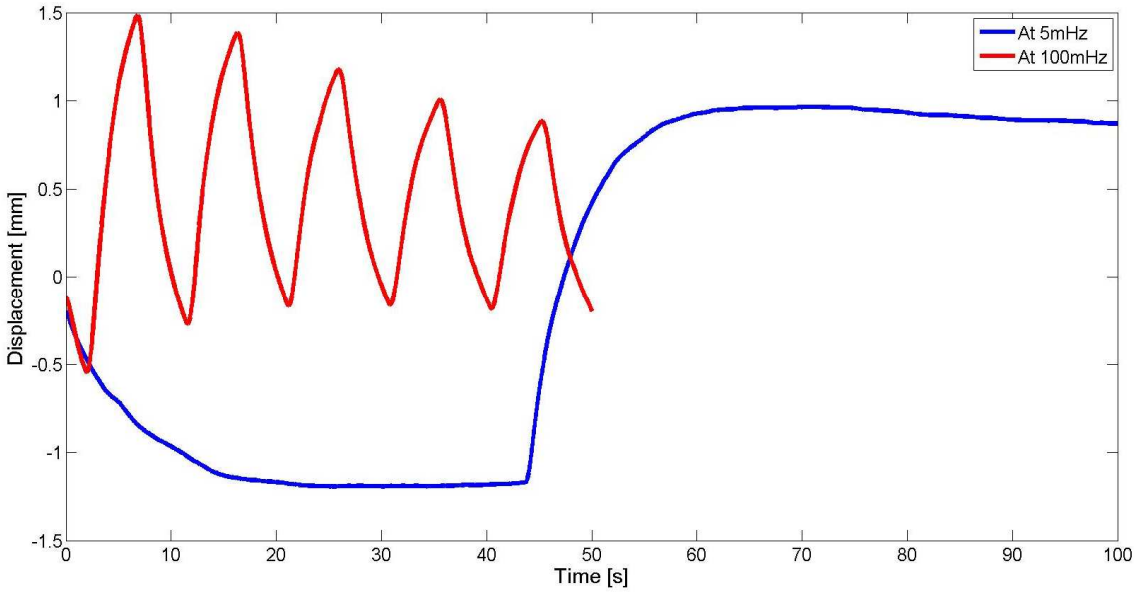

Figure 51: Graph representing displacement of the actuator tip in millimetres versus the time of actuation for an actuator of 0.22mm of thickness. Each line is representing a different frequency. Only five cycles are shown for actuation at 100mHz.

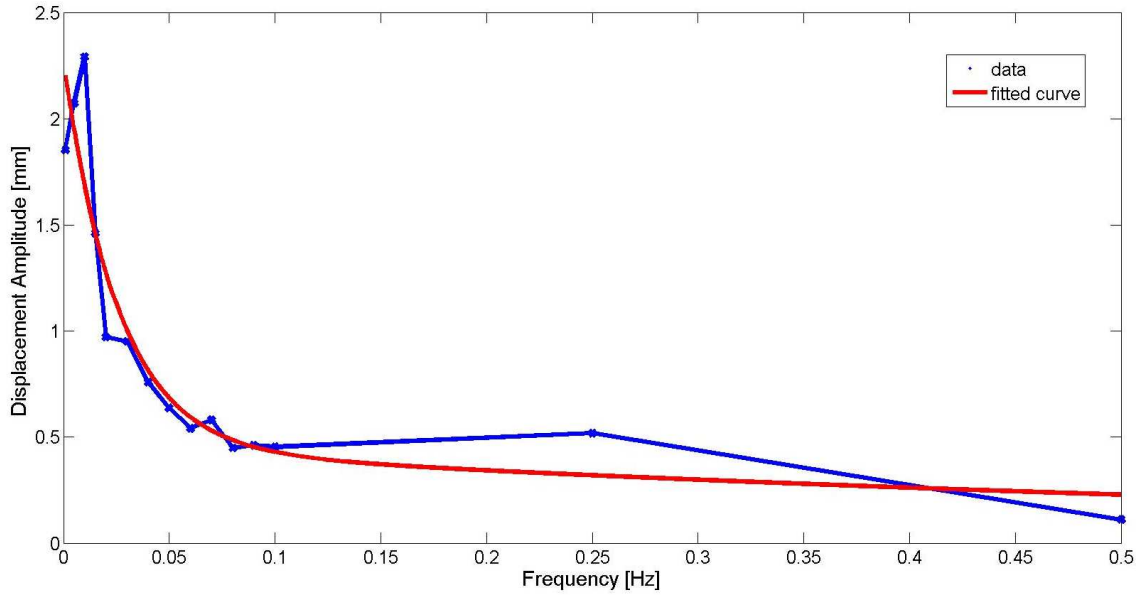

Figure 52: Tip deflection amplitude for an actuator of 0.22mm thickness. Actual data can be seen in the blue curve. The red curve is a fitted curve of all the values.

6.2.3. Sample length variation

In this study, the variation of the actuator length is considered. Three specimens of the same width and thickness are used, but with lengths of 10, 13 and 15mm long

respectively. Data about the specimens and the conditions for actuation are recorded in *Table 17*.

Table 17: Specimens size and data about actuation for the comparative study of three different actuator lengths.

Parameter	Specimen 1	Specimen 2	Specimen 3
Size [mm]	10.01x3.91x0.09	13.20x4.08x0.10	15.01x4.14x0.10
Relative humidity [%]	36	46	45
Actuation Voltage [V]	10	10	10
Actuation Frequency [Hz]	0.008	0.008	0.008

In *Figures 53* and *54* results are shown displaying the tip displacement of the three specimens versus time and the tip displacement amplitude of each specimen per cycle.

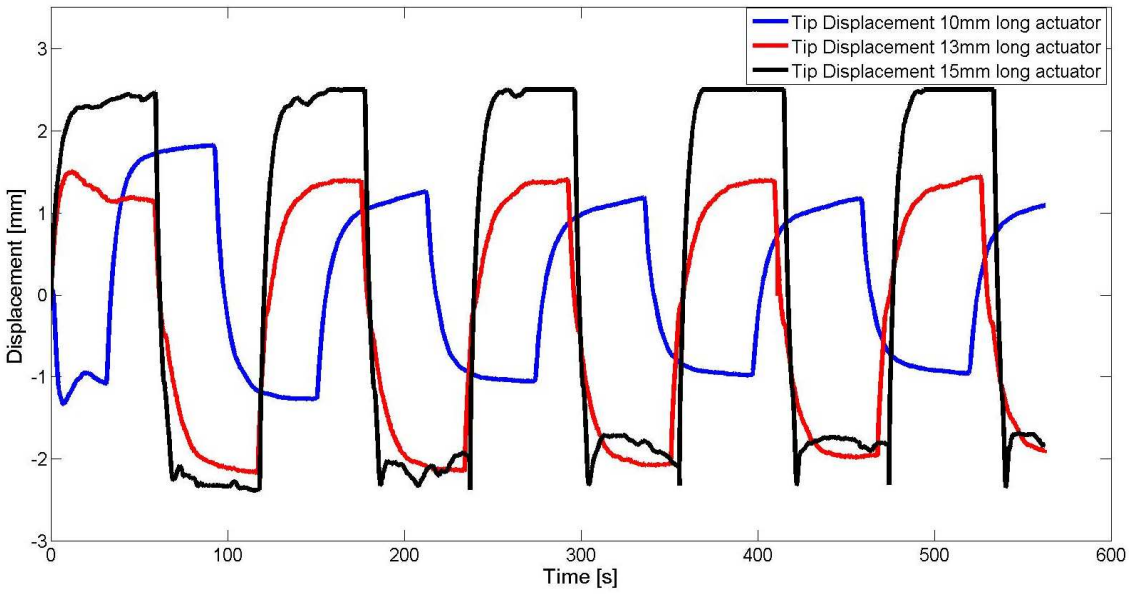

Figure 53: Tip displacement for three different actuators with varying lengths (10, 13 and 15mm) subjected to a 10V electric periodic signal at 0.008Hz.

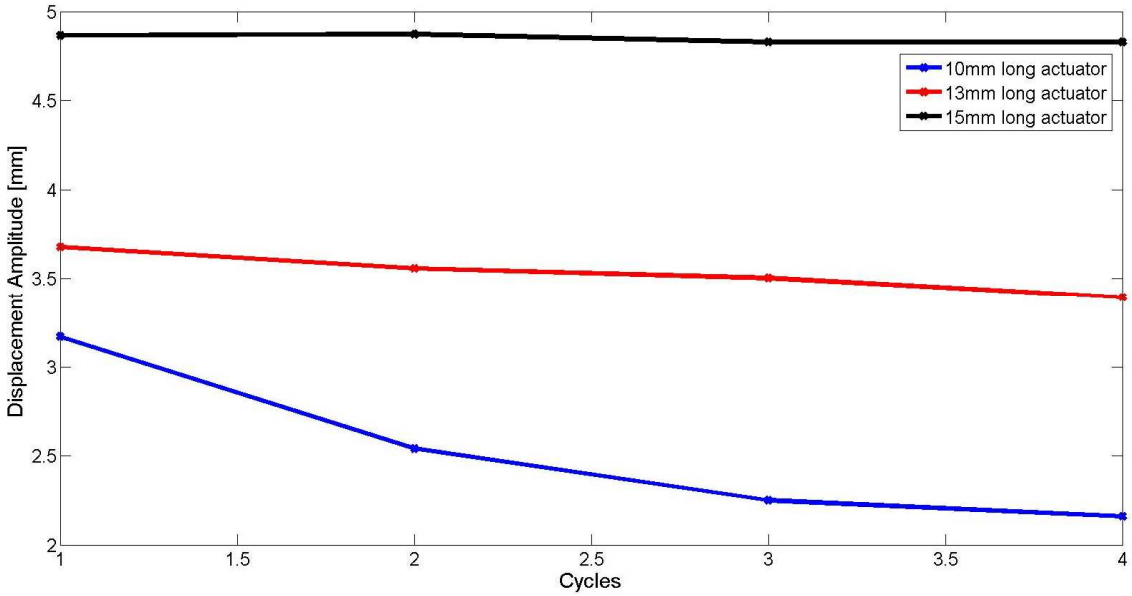

Figure 54: Tip displacement amplitude for three different actuators with varying lengths (10, 13 and 15mm) subjected to a 10V electric periodic signal at 0.008Hz.

With these two last figures (*Figures 53* and *54*) we can see that the longer the actuator (provided same thickness and width) the higher the value for displacement amplitude.

6.2.4. Fatigue behaviour

To subject the specimens to actuation fatigue, squared waves were also used as an electrical input. The material was actuating during a very long time (between 8 and 24h) at the same conditions, which are in fact detailed in *Table 18*.

Table 18: Specimens data about fatigue actuation behaviour.

Parameter	Value
Voltage [V]	5
Frequency [Hz]	0.008
Humidity	25±5%
Time acquisition interval [s]	1

Other values were also recorded for each case such as the size and initial and final mass. Mass was considered relevant in case the actuator lose a significant amount since it would have been due to water loss during actuation. However, in any specimen tasted the mass lost was not over a 1% of the initial mass.

The main aim of this study was to assess the long time performance of the actuator in terms of displacement amplitude variation over time. Several specimens were tried with similar sizes and also varying thickness. As a wide amount of data was collected for each test, for ease of data processing, only the first eight hours were considered. Results were all alike and similar to *Figure 55*.

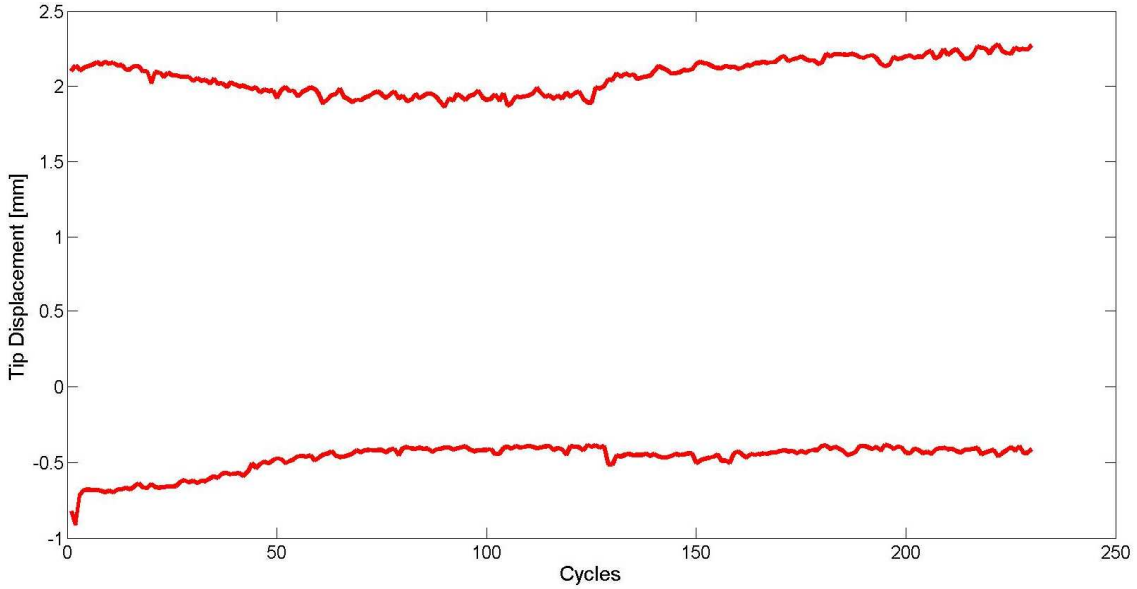

Figure 55: Maximum tip displacement to anode and cathode of an actuator subjected to actuation fatigue over 8h (240 cycles). It shows an initial decrease in the amplitude of the tip displacement.

As *Figure 55* shows, there is an initial decrease in the amplitude of the tip displacement, but in general, it can be assumed to be constant over time. After such a long time actuating, there is no worsening of the actuation displacement of the IPMC.

6.2.5. Long time exposure to a constant voltage

In this case, no periodic signal was used as an electric input for actuation. A constant electric supply was indeed used to study if the IPMC suffers bending relaxation after a certain amount of time.

This test was performed in specimens of the three thicknesses i.e. 0.10, 0.17 and 0.22mm during an hour. A current of 5V was supplied. More information about each specimen and test is given in *Table 19*.

Table 19: Actuation parameters to study the long time exposure to a constant voltage of the IPMC actuator for a voltage of 5V.

Specimen	Length [mm]	Width [mm]	Thickness [mm]	Relative humidity [%]	Voltage [V]
1	10	4.17	0.10	23.2	5
2	10	3.90	0.17	22.6	5
3	10	4.06	0.22	23.5	5

Data is collected in Excel sheets and loaded to Matlab to be processed. A comparative graph is built and showed in *Figure 56*. Results for the IPMCs with thicknesses of 0.17 and 0.22mm show a compliant behaviour: the thicker IPMC has a lower displacement than the 0.17mm one and, moreover, both actuators show some bending relaxation over time, i.e. a 27.5% relaxation for the 0.22mm thickness actuator and a 30.5% for the 0.17mm one. However, when coming to the 0.1mm thickness IPMC, it increases bending over time and the tip displacement should be higher than for the other two cases. No explanation for this issue is conceived.

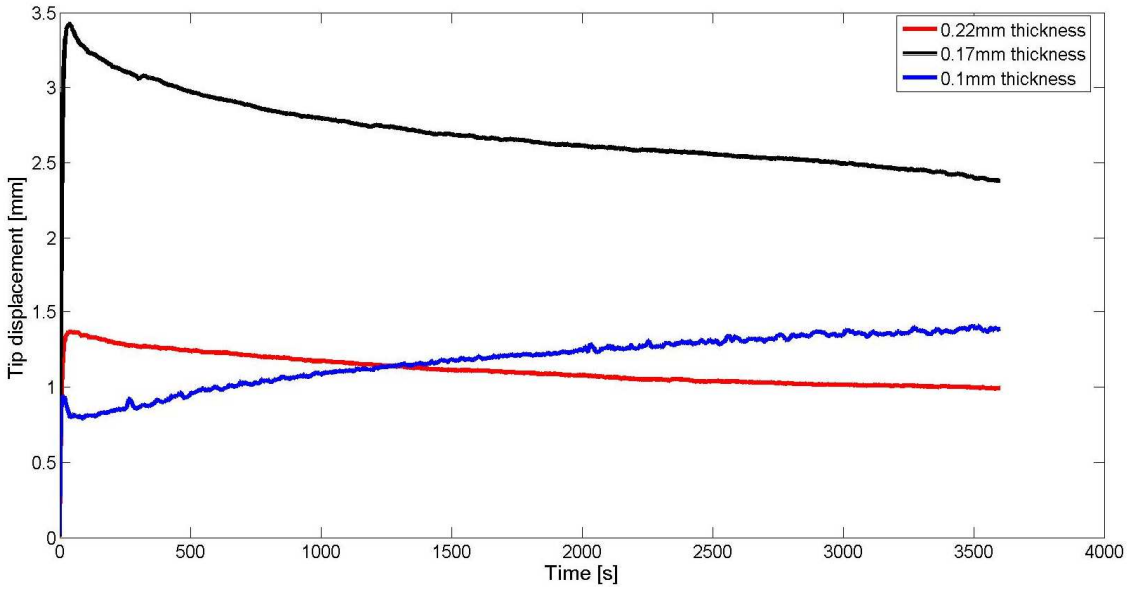

Figure 56: Graph representing the tip displacement of three IPMC actuators of 0.1, 0.17 and 0.22mm thick at a constant voltage of 5V during an hour. Behaviour of the 0.1mm specimen seems to be different, increasing the tip deflection with time, instead of decreasing, as the other two specimens show.

6.3. Summary of the results obtained

Several tests were performed to select the IPMC processing conditions. The used lay-up for the hot-plate press processing consisted of Teflon sheets sandwiching the fluoropolymer pellets for them not to stick to the press plates. Metal bands (shims) of a certain thickness were also used framing the pellets to control the desired thickness. When talking about the temperature profile, it has been demonstrated that an appropriate treatment is achieved at a maximum temperature of 200ºC, with temperature ramps of 10ºC/min and -3ºC/min to avoid fast cooling and stretch marks that affect negatively to material properties. Pressure was found to be adequate at 25kN.

In the preparation and preliminary testing of the IPMC as an actuator, contrary to what is reported by many authors, it has been found that the IPMC does not to need to be soaked in a solution or in water for it to actuate, the sole contribution of the ambient humidity permits actuation and therefore plays an important role in the whole procedure.

A tensile test in an INSTRON machine was also performed to measure the strength capabilities of the material. Scanning electron microscopy was also used for material characterization.

When talking about actuation, aforementioned results show that it depends on several factors: length and thickness of the specimen, voltage supply, frequency of the supplied signal or overall time of actuation.

- When polarity of the supplied signal changes, so does bending of the actuator. The actuator is found to bend towards the anode, so when polarity changes, the actuator bends towards the other side.
- The longer the specimen, the higher the tip displacement.
- The thicker the specimen, the higher the tip displacement.
- The higher the voltage, the higher the tip displacement, up to a voltage value where the specimen seems to degrade and lose its actuation properties (around 12-15V).

- The higher the frequency of the supplied signal, the lower the tip displacement because the actuator does not have time enough to achieve its maximum deflection.
- When a specimen is subjected to a constant voltage (frequency=0Hz), it has been found that the actuation displacement normally decreases with time i.e. it suffers bending relaxation .
- When a specimen is subjected to a cyclic voltage supply (frequency>0Hz) for a long time, the tip displacement amplitude slightly decreases after about 1h of actuation.

7. Conclusion and recommendations for future work

In this project it has been studied the behaviour of an electroactive polymer (fluoropolymer) as a electrolyte membrane of an ionic polymer-metal composite (IPMC) actuator. The material has been simple processed into layers using a hot-plate press and coated on both sides with gold electrodes. The IPMC shows bending deformation when being connected to an electric current in a cantilever configuration. The purpose of this study was to better understand the actuation mechanism of the IPMC as well as important factors that may drive or affect actuation.

A rapid actuation was found at low values of driving voltage, which means a safer alternative to conventional actuators for medical applications. Properties are found to be similar or better than in other electroactive polymer actuators or in conventional actuators.

Due to the lack of information on this topic and the great amount of parameters involved in actuation of the fluoropolymer, it has been very difficult to fully understand and use the material efficiently. Actuators have shown very diverse and non-repetitive results, making it complicated to control the amount of actuation deflection or the voltage required to achieve a certain displacement.

For future studies or work in this topic, it would be very interesting to go in depth the physicochemical fundamentals behind the actuation mechanism of these kind of materials, since water seems to be an essential element and the ion that moves within the electrolyte membrane is still unknown. Once this mechanism is fully understood, more complex actuation mechanisms and structures will be developed, showing better material properties and very interesting potential applications.

It would also be very interesting to measure the blocking force of this material, and how it varies with the specimen geometry and actuation voltage. Correlating measurements and results one could also apply formulas to model the deformation of the actuator. For this purpose, more repetitive results need to be achieved. Understanding the whole mechanism better will enable a repetitive and controlled use of the actuator.

As a final conclusion for this project, it has been found an alternative and cheaper way of producing an IPMC from a fluoropolymer membrane, with the novelty of no ionic liquid or direct method for humidification other than ambient humidity.

8. References

Bar-cohen, Yoseph. 2004. “Electroactive Polymers (EAP) as Actuators for Potential Future Planetary Mechanisms.” In *NASA/DoD Conference on Evolution Hardware*, 1–9. Pasadena (CA).

Bar-Cohen, Yoseph, and Sean Leary. 2000. “ELECTROACTIVE POLYMERS AS ARTIFICIAL MUSCLES CHANGING ROBOTICS PARADIGMS.” In *National Space and Missile Materials Symposium*. Pasadena (CA).

Bar-Cohen, Yoseph, and Qiming Zhang. 2008. “Electroactive Polymer Actuators and Sensors” 33 (March): 173–81.

Bautista-Rodríguez, C .Moisés, Araceli Rosas-Paleta, J. Antonio Rivera-Márquez, and Omar Solorza-Feria. 2009. “Study of Electrical Resistance on the Surface of Nafion 115 ® Membrane Used as Electrolyte in PEMFC Technology Part I : Statistical Inference.” *International Journal of Electrochemical Science* 4: 43–59.

Bennett, M. D., and D. J. Leo. 2003. “Manufacture and Characterization of Ionic Polymer Transducers Employing Non-Precious Metal Electrodes.” *Smart Materials and Structures* 12: 424–36. stacks.iop.org/SMS/12/424.

Bhandari, Binayak, Gil-Yong Lee, and Sung-Hoon Ahn. 2012. “A Review on IPMC Material as Actuators and Sensors: Fabrications, Characteristics and Applications.” *International Journal of Precision Engineering and Manufacturing* 13 (1): 141–63. doi:10.1007/s12541-012-0020-8.

Boyle, N. G., V. J. McBrierty, and A. Eisenberg. 1983. “NMR Investigation of Molecular Motion in Nafion Membranes.” *Macromolecules* 16 (1): 80–84.

Calvert, Paul. 2008. “Gel Sensors and Actuators.” *MRS Bulletin* 33 (March).

Cheng, Zhongyang, and Qiming Zhang. 2008. “Field-Activated Electroactive Polymers” 33 (MRS Bulletin): 183–87.

Cottinet, Pierre-jean, Daniel Guyomar, Benoit Guiffard, Laurent Lebrun, and Chatchai Putson. 2004. “Electrostrictive Polymers as High-Performance Electroactive Polymers for Energy Harvesting,” 185–209.

Cottrell, T. L. 1958. *The Strengths of Chemical Bonds*. 2nd ed. Butterworth, London.

Doam, Ngoc Chi Nam, and Kyoung Kwan Ahn. 2012. “Ionic Polymer Metal Composite Transducer and Self-Sensing Ability.” In *Smart Actuation and Sensing Systems - Recent Advances and Future Challenges*, edited by Giovanni Berselli, Rocco Vertechy, and Gabriele Vassura. doi:10.5772/51310.

Eisenberg, A., and J. S. Kim. 1996. "Ionomers (Overview)." *Polymeric Materials Encyclopedia*, 3435–54.

Gautschi, Gustav. 2002. *Piezoelectric Sensorics: Force, Strain, Pressure, Acceleration and Acoustic Emission Sensors, Materials and Amplifiers*. Berlin: Springer.

Gebel, G. 2000. "Structural Evolution of Water Swollen Perfluorosulfonated Ionomers from Dry Membrane to Solution." *Polymer* 41: 5829–38.

Gebel, G., and R. B. Moore. 2000. "Small-Angle Scattering Study of Short Pendant Chain Perfluorosulfonated Ionomer Membranes." *Macromolecules* 33 (13): 4850–485.

Goulbourne, Nakhiah C. S. 2005. "ELECTROELASTIC MODELING OF DIELECTRIC ELASTOMER MEMBRANE ACTUATORS." The Pennsylvania State University.

Harwin, W S, W Hayes, G Jeronimidis, and G R Mitchell. 2004. "EAP-BASED ARTIFICIAL MUSCLES AS AN ALTERNATIVE TO SPACE MECHANISMS," no. 18151: 1–51.

Hong, Wangyujue, Abdallah Almomani, and Reza Montazami. 2014. "Influence of Ionic Liquid Concentration on the Electromechanical Performance of Ionic Electroactive Polymer Actuators." *Organic Electronics* 15 (11). Elsevier B.V.: 2982–87. doi:10.1016/j.orgel.2014.08.036.

Ieda, Masayuki. 1980. "Dielectric Breakdown Process." *Transactions of Electrical Insulation* EI-15 (3): 206–24.

James, P. J., T. J. McMaster, J. M. Newton, and M. J. Miles. 2000. "In Situ Rehydration of Perfluorosulphonate Ion-Exchange Membrane Studied by AFM." *Polymer* 41: 4223–31.

Kestelman, V N, L S Pinchuk, and V A Goldade. 2000. *Electrets In Engineering: Fundamentals and Applications*. Springer US. http://books.google.es/books?id=exF0dkjju1UC.

Kim, Doyeon, Kwang J. Kim, Jae Do Nam, and Viljar Palmre. 2011. "Electro-Chemical Operation of Ionic Polymer-Metal Composites." *Sensors and Actuators, B: Chemical* 155 (1). Elsevier B.V.: 106–13. doi:10.1016/j.snb.2010.11.032.

Ko, Wen-Ching, Kuan-Wei Chen, Chang-Ho Liou, Yu-Chi Chen, Wen-Jong Wu, and Chih-Kung Lee. 2012. "Study and Application of Free-Form Electret Actuators." *IEEE Transactions on Dielectrics and Electrical Insulation* 19 (4): 1226–33. doi:10.1109/TDEI.2012.6259995.

Kornbluh, Roy, Ron Pel, Joseph Eckerle, and Jose Joseph. 1998. "ELECTROSTRICTIVE POLYMER ARTIFICIAL MUSCLE ACTUATORS." *Internationla Conference on Robotics and Automation*, no. May: 2147–54.

Kosidlo, U, M Omastová, M Micusík, G Ćirić-Marjanović, H Randriamahazaka, T Wallmersperger, A Aabloo, I Kolaric, and T Bauernhansl. 2013. "Nanocarbon Based Ionic Actuators—a Review." *Smart Materials and Structures* 22 (10): 1–30. doi:10.1088/0964-1726/22/10/104022.

Kumar, S Mukesh, and M Vanitha Lakshmi. 2013. "APPLICATIONS OF SHAPE MEMORY ALLOYS IN MEMS DEVICES" 2 (2): 1122–27.

Lee, Deuk Yong, Il Seok Park, Myung Hyun Lee, Kwang J. Kim, and Seok Heo. 2007. "Ionic Polymer-Metal Composite Bending Actuator Loaded with Multi-Walled Carbon Nanotubes." *Sensors and Actuators, A: Physical* 133 (1): 117–27. doi:10.1016/j.sna.2006.04.005.

Lee, Je Seung, Nguyen Dinh Quan, Jung Min Hwang, Sang Deuk Lee, Honggon Kim, Hyunjoo Lee, and Hoon Sik Kim. 2006. "Polymer Electrolyte Membranes for Fuel Cells.pdf." *Industrial and Engineering Chemistry* 12 (2): 175–83.

Lee, Soon-gie, Hoon-cheol Park, Surya D Pandita, and Youngtai Yoo. 2006. "Performance Improvement of IPMC (Ionic Polymer Metal Composites) for a Flapping Actuator." *International Journal of Control, Automation and Systems* 4 (6): 748–55.

Lévy, Élie. 2008. *Diccionario Akal de Física*. 3rd ed. Tres Cantos: Akal.

Liu, Sheng, Yang Liu, Hülya Cebeci, Roberto Guzmán De Villoria, Jun Hong Lin, Brian L. Wardle, and Q. M. Zhang. 2010. "High Electromechanical Response of Ionic Polymer Actuators with Controlled-Morphology Aligned Carbon Nanotube/nafi on Nanocomposite Electrodes." *Advanced Functional Materials* 20 (19): 3266–71. doi:10.1002/adfm.201000570.

MacFarlane, Douglas R., Naoki Tachikawa, Maria Forsyth, Jennifer M. Pringle, Patrick C. Howlett, Gloria D. Elliott, James H. Davis, Masayoshi Watanabe, Patrice Simon, and C. Austen Angell. 2014. "Energy Applications of Ionic Liquids." *Energy & Environmental Science* 7 (1): 232–50. doi:10.1039/c3ee42099j.

Madden, J.D.W., N.a. Vandesteeg, P.a. Anquetil, P.G.a. Madden, a. Takshi, R.Z. Pytel, S.R. Lafontaine, P.a. Wieringa, and I.W. Hunter. 2004. "Artificial Muscle Technology: Physical Principles and Naval Prospects." *IEEE Journal of Oceanic Engineering* 29 (3): 706–28. doi:10.1109/JOE.2004.833135.

Madden, John D. 2004. "Actuator Selection for Variable Camber Foils." Edited by Yoseph Bar-Cohen. *Smart Structures and Materials* 5385 (May 2011): 442–48. doi:10.1117/12.546151.

NASA. 2014. "Electroactive Polymers 1: Piezoelectric Materials." *Aviation Research*. Accessed October 1. http://quest.arc.nasa.gov/aero/virtual/demo/research/youDecide/piezoElectMat.html.

Nguyen, Vinh Khanh, Jang Woo Lee, and Youngtai Yoo. 2007. "Characteristics and Performance of Ionic Polymer – Metal Composite Actuators Based on Nafion / Layered Silicate and Nafion / Silica Nanocomposites." *Sensors and Actuators B: Chemical* 120 (2): 529–37. doi:10.1016/j.snb.2006.03.015.

Nouel, Karine M, and Peter S Fedkiw. 1998. "Nafion-Based Composite Polymer Electrolyte Membranes" 43 (97).

Öner, Erhan. 2007. "Uzaktan Egitim Platformu." *Thermogravimetric Analysis (TGA)*. http://www.uzaktanegitimplatformu.com/UEP/uep_ylisans/ey2/ey2_download/Practice Guide_Section 2_TGA.pdf.

Opekar, Frantisek, and Karel Stulik. 1999. "Electrochemical Sensors with Solid Polymer Electrolytes." *Analytica Chimica Acta* 385: 151–62.

Opekar, Frantisek, and Daniel Svozil. 1995. "Electric Resistance in a Nafion ® Membrane Exposed to Air after a Step Change in the Relative Humidity" 117 (29): 5–7.

Orfino, F. P., and S. Holdcroft. 2000. "The Morphology of Nafion: Are Ion Clusters Bridged by Channels or Single Ionic Sites?" *Journal of New Materials for Electrochemical Systems* 3 (4): 285–90.

Park, Il-Seok, Kwangmok Jung, Doyeon Kim, Sang-mun Kim, and Kwang J Kim. 2008. "Physical Principles of Ionic Polymer – Metal Composites as Electroactive Actuators and Sensors" 33 (March).

Pelrine, Ronald E, Roy D Kornbluh, and Jose P Joseph. 1998. "Electrostriction of Polymer Dielectrics with Compliant Electrodes as a Means of Actuation" 64 (97): 77–85.

Perma Pure LLC. 2014. "Perma Pure: Making Analysis Possible." *All about Nafion*. Accessed November 21. http://www.permapure.com/.

Pillai, Priam Vasudevan. 2011. "Development and Characterization of Conducting Polymer Actuators by Accepted by ....." Massachusetts Institute of Technology. http://dspace.mit.edu/handle/1721.1/67594.

Pineri, M., F. Volino, and M. Escoubes. 1985. "Evidence for Sorption-Desorption Phenomena During Thermal Cycling in Highly Hydrated Perfluorinated Membranes." *Journal of Polymer Science: Polymer Physics* 23 (10): 2009–20.

Rubalcaba Sánchez, Juan Carlos. 2015. "Músculo Artificial Basado En Polímero Electroactivo Y Su Aplicación En Robótica." Carlos III de Madrid.

Scott, Chris E. 2001. "Polymer Processing." http://www.polymerprocessing.com/.

Shahinpoor, M, J O Simpson, and J Smith. 1998. “Ionic Polymer – Metal Composites (IPMCs) as Biomimetic Sensors , Actuators and Artificial Muscles — a Review.” *Smart Materials and Structures* 15 (7): R15–30.

Shahinpoor, M. 1991. “Conceptual Design , Kinematics and Dynamics of Swimming Robotic Structures Using Ionic Polymeric Gel Muscles.” *Smart Materials and Structures* 1: 91–94.

Shaw, Robert. 2014. “Ferroelectric Materials.” *DoITPoMS, University of Cambridge*. Accessed November 3. http://www.doitpoms.ac.uk/tlplib/ferroelectrics/printall.php.

TA Instruments. 2012a. “THERMAL ANALYSIS.” *Q500 & Q50 Thermogravimetric Analysis Brochure*.

———. 2012b. “THERMAL ANALYSIS:” *Q2000 Differential Scanning Calorimeter Brochure*.

Terasawa, Naohiro, Ichiroh Takeuchi, Hajime Matsumoto, Ken Mukai, and Kinji Asaka. 2011. “High Performance Polymer Actuator Based on Carbon Nanotube-Ionic Liquid Gel: Effect of Ionic Liquid.” *Sensors and Actuators B: Chemical* 156 (2). Elsevier B.V.: 539–45. doi:10.1016/j.snb.2010.09.009.

Tiwari, R, and E Garcia. 2011. “The State of Understanding of Ionic Polymer Metal Composite Architecture: A Review.” *Smart Materials and Structures* 20 (8). doi:10.1088/0964-1726/20/8/083001.

Uchida, Mikio, and Minoru Taya. 2001. “Solid Polymer Electrolyte Actuator Using Electrode Reaction” 42: 9281–85.

Uchino, Kenji. 1995. “Advances in Ceramic Actuator Materials.” *Materials Letters* 22 (January): 1–4.

University, McGill. 2014. “NanoScience & Scanning Probe Microscopy.” *Microcantilever-Based Sensors*. Accessed November 5. http://www.physics.mcgill.ca/~SPM/sensor/ppyexpt.htm.

Van den Bossche, N. 2006. *Polymer Characterization Tests (DSC, TGA, GPC)*.

Vatansever, D., E. Siores, and T. Shah. 2012. “Alternative Resources for Renewable Energy: Piezoelectric and Photovoltaic Smart Structures.” In *Global Warming-Impacts and Future Perspective*, edited by Bharat Raj Singh. doi:10.5772/50570.

Yeom, Sung-Weon, and Il-Kwon Oh. 2009. “A Biomimetic Jellyfish Robot Based on Ionic Polymer Metal Composite Actuators.” *Smart Materials and Structures* 18 (8): 085002. doi:10.1088/0964-1726/18/8/085002.

Yoshida, Hiroshisha, and Yuka Miura. 1992. “Behavior of Water in Perfluorinated Ionomer Membranes Containing Various Monovalent Cation.” *Journal of Membrane Science* 68 (1): 1–10.

Yoshida, Ryo, Takamasa Sakai, Yusuke Hara, Shingo Maeda, Shuji Hashimoto, Daisuke Suzuki, and Yoko Murase. 2009. “Self-Oscillating Gel as Novel Biomimetic Materials.” *Journal of Controlled Release* 140 (3). Elsevier B.V.: 186–93. doi:10.1016/j.jconrel.2009.04.029.

Yun, Gyu-young, Heung Soo Kim, and Jaehwan Kim. 2008. “Blocked Force Measurement of an Electro-Active Paper Actuator Using a Cantilevered Force Transducer.” *Smart Materials and Structures* 17 (2).

Zeus Industrial Products Inc. 2006. “Cole-Parmer.” *Chemical Resistance of Fluoropolymers*. http://www.coleparmer.com/TechLibraryArticle/827.

Appendix I: Bond dissociation energy for various bond types

C-F and C-C bonds are very stable and hard to break. In general, these are the bonds which characterize the molecular structure of fluoropolymers together with C-H (not present in this case). Data for bond dissociation energy, amount of energy released when a bond is broken, is tabulated for further information about this topic i.e. the higher the bond dissociation energy, the more difficult would be breaking that particular bond.

Table 20: Bond dissociation energy for examples containing carbon and several other elements (Cottrell, 1958). The bond dissociation energy is the amount of energy released when a bond is broken. The higher the bond dissociation energy, the more difficult would be breaking that particular bond.

Bond	Bonds dissociation energy [kJ/mol]
C-F	536
C-C	607
C-I	209
C-H	337.2

Appendix II: Additional information about DSC

DSC is a technique that consist in measuring the temperature difference between two cells, one of which is the reference cell (T_R) and the other one contains the sample to study (T_S). By making a prior calibration of the equipment, the equipment thermal resistance can be determined (dU_S) and the temperature difference can be translated into heat flux following *Equation 1*. Calibration depends on the gas used for purging and is already done for helium, nitrogen, air and oxygen. However, parameters for calibration can be changed in order to use other gases.

$$Heat\ flux = \frac{T_S - T_R}{dU_S} \quad (1)$$

DSC requires the previous specification of a temperature treatment with information regarding the sampling interval, initial temperature, one or several temperature maximums/minimums, temperature ramps, etc.

DSC exposes both capsules to a programmed thermal treatment and temperature is measured separately for each one. When analysing the temperature for the reference capsule, it can be seen that it will be a bit lower than the specified temperature because the capsule absorb some heat (capsule calorific capacity or C_p). Temperature will be even lower for the sample capsule because heat will be absorbed by the capsule and also by the sample inside. Since capsules are identical, the temperature difference between them is proportional to the calorific capacity C_p of the sample. Temperature is translated into heat flux. At the end, what it is obtained is a graph relating heat flux versus temperature.

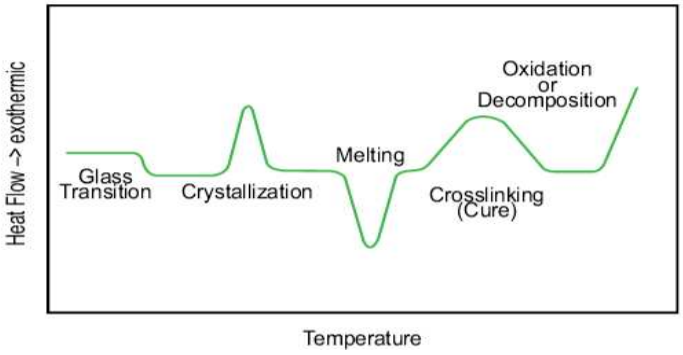

Figure 57: Characteristic graph for a Differential Scanning Calorimeter (DSC) (TA Instruments, 2012a) relating heat flow with temperature. Study is carried on comparing two cells (a reference cell and another one

containing the material of interest). Characteristic transitions for polymers are shown. Exothermic reactions are depicted with 'positive' variations, whereas endothermic by 'negative' variations.

- Straight line: If no transition has taken place, temperature difference between both cells will be constant and equal to a value proportional to the calorific capacity of the sample material.
- Glass Transition Temperature (T_g): it is a second order transition or, in other terms, it involves just the change in calorific capacity, not in the material latent heat[5]. The calorific capacity of a material in glass state is different from the one that it will manifest above its T_g. In DSC curve, it will be represented by a sudden jump.
- Melting point: during melting temperature does not change but materials absorb heat (latent heat) that is used to break the polymer crystalline structure. It is an endothermic process. Hence, an endothermic peak is shown to appear to represent this transition.
- Crystallization: the same concept for melting point can be applied for crystallization but the other way around. Crystallization is an exothermic transition that release heat when occurring. Temperature is also observed to remain constant and, therefore, an exothermic peak appears.

[5] Energy needed for a material to change phase from solid to liquid or form liquid to gas. This energy is just invested for phase change, not for energy increase.

Appendix III: Additional information about TGA

Thermo-gravimetric analysis is a technique where the mass of a material sample is recorded as a function of the temperature or as a function of time while it is subjected to a specified thermal treatment. Samples are placed inside a sample pan that is hanging from a balance. The pan is situated inside a furnace, which is in charge of heating or cooling the sample during the experiment. The balance measures very precisely the change in mass of the sample while the experiment is being carried out. The furnace environment can be controlled by flow of an specific gas around the sample and out of the furnace. If an inert atmosphere (using argon or helium) is used during heating, the material will only react to temperature during decomposition.

Using TGA analysis it is possible to assess the loss of any kind of solvent or water, oxidation or decomposition of the material, amount of carbon within the material, amount of filler lost or amount of ash remaining at the end of the process, among other parameters (Van den Bossche, 2006).

TGA also needs to be calibrated prior to use. Buoyancy effects may have significant effects on the sample if calibration is not done properly. The density of the purge gas may vary with temperature and this factor needs to be accounted for when performing the study. In order to properly design the temperature profile, the maximum temperature should be high enough so that the material has completed all chemical reactions and the weight becomes stable (Öner, 2007).

Appendix IV: Results for INSTRON tensile test for 8 different specimens of EAP.

Table 21: Results for Young's modulus, maximum load, maximum stress and maximum strain from the INSTRON tensile test for 8 different specimens.

Specimen	Young's Modulus [MPa]	Max Stress [MPa]	Max Strain [mm/mm]
1	196.0474	15.5843	0.3737
2	189.3337	19.1751	0.3940
3	166.5889	17.5972	0.4427
4	94.8670	19.1790	0.5855
5	209.7514	17.1599	0.2289
7	138.1877	15.8021	0.4801
8	226.3208	16.9245	0.3955
9	225.6767	16.0336	0.2500
Mean	180	17.1	0.39
Standard Deviation	45	1.4	0.12

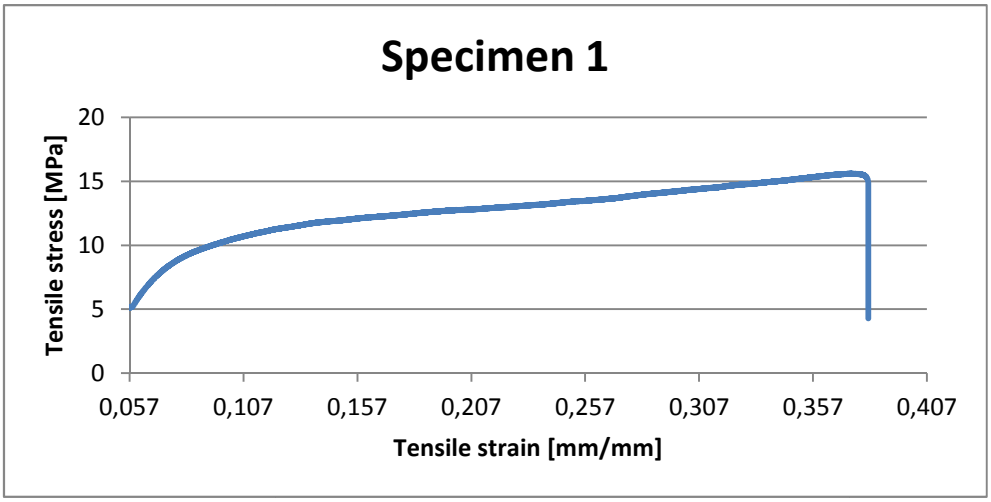

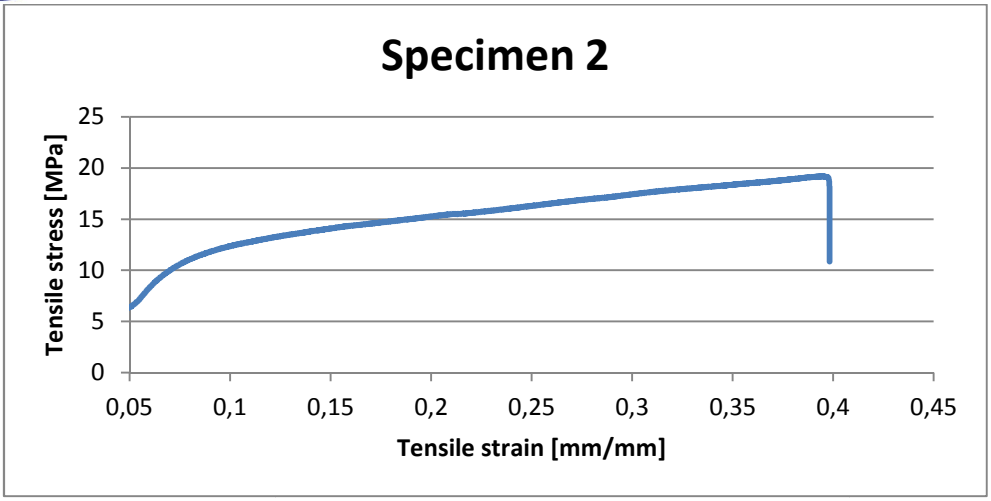
Specimen 2
Tensile stress [MPa]
25
20
15
10
5
0
0,05
0,1
0,15
0,2
0,25
0,3
0,35
0,4
0,45
Tensile strain [mm/mm]

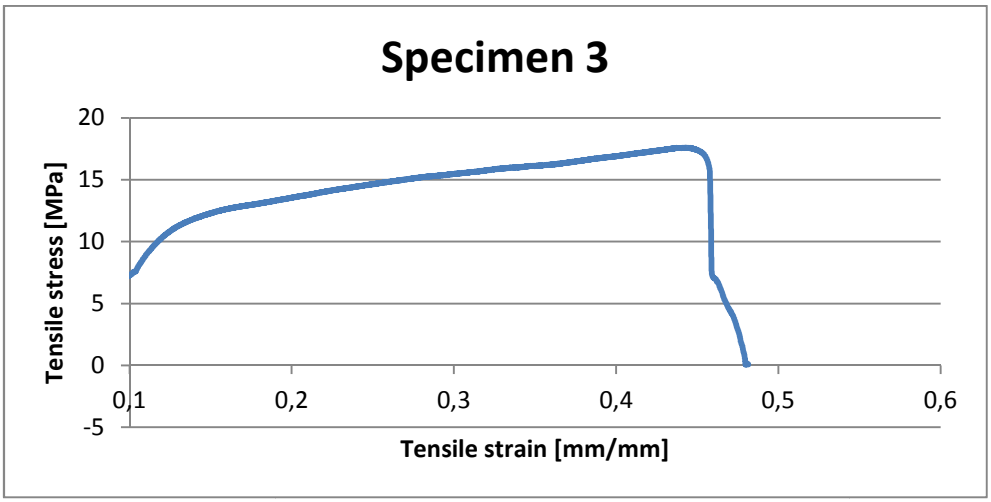
Specimen 3
Tensile stress [MPa]
20
15
10
5
0
-5
0,1
0,2
0,3
0,4
0,5
0,6
Tensile strain [mm/mm]

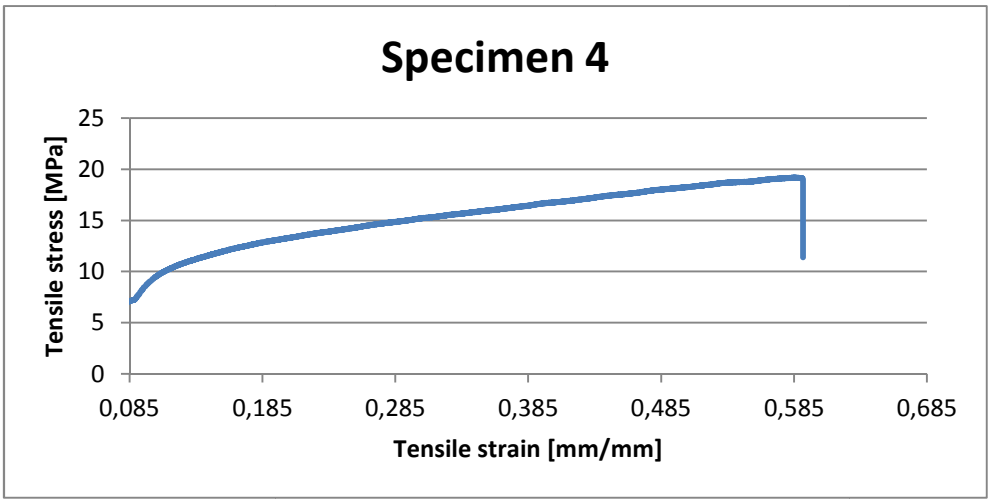
Specimen 4
Tensile stress [MPa]
25
20
15
10
5
0
0,085
0,185
0,285
0,385
0,485
0,585
0,685
Tensile strain [mm/mm]

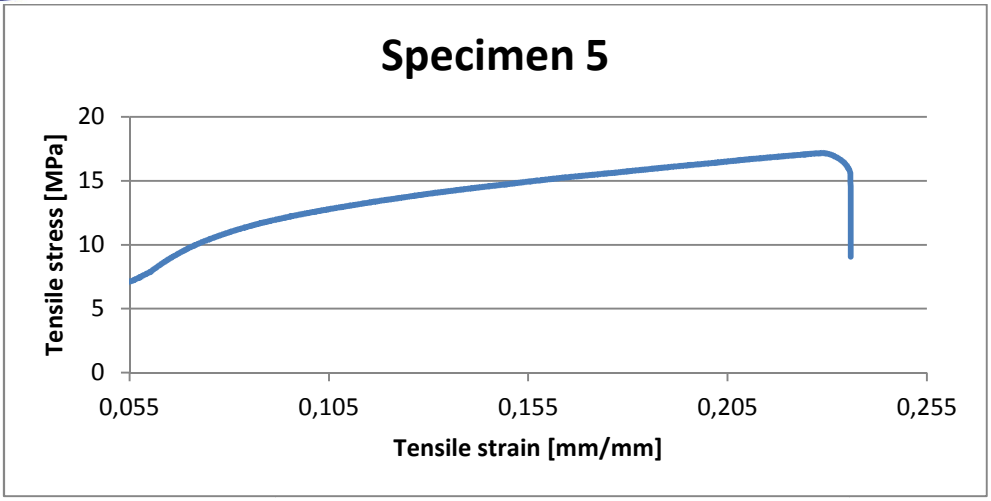
Specimen 5
Tensile stress [MPa]
20
15
10
5
0
0,055
0,105
0,155
0,205
0,255
Tensile strain [mm/mm]

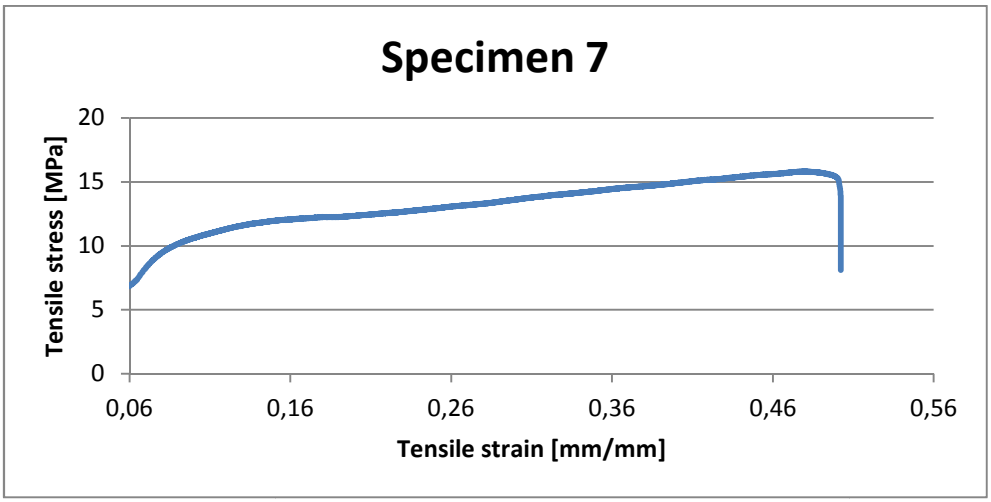
Specimen 7
Tensile stress [MPa]
20
15
10
5
0
0,06
0,16
0,26
0,36
0,46
0,56
Tensile strain [mm/mm]

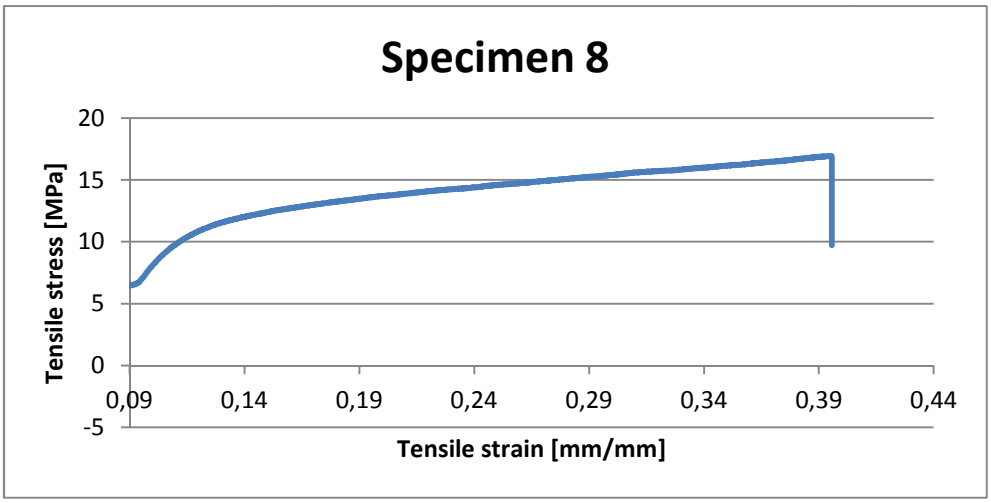
Specimen 8
Tensile stress [MPa]
20
15
10
5
0
-5
0,09
0,14
0,19
0,24
0,29
0,34
0,39
0,44
Tensile strain [mm/mm]

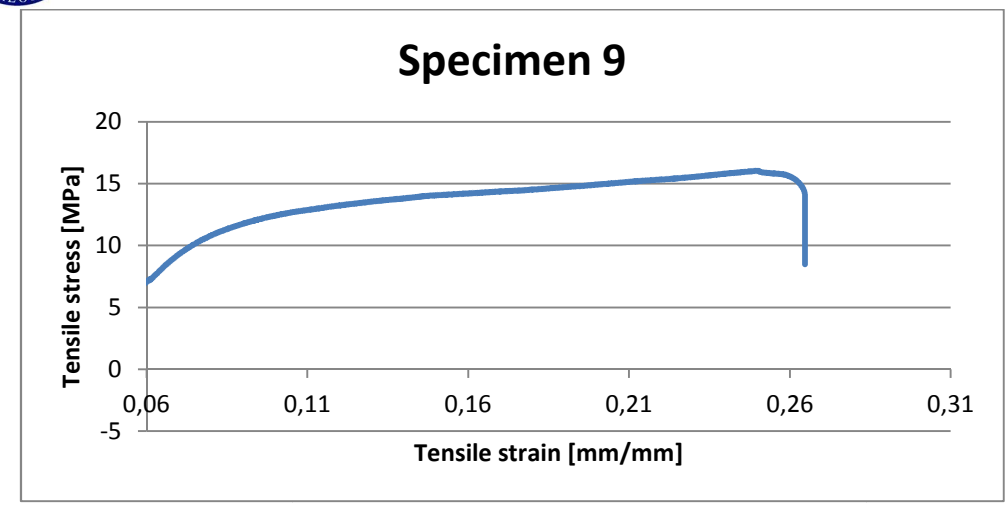
Specimen 9
Tensile stress [MPa]
20
15
10
5
0
-5
0,06
0,11
0,16
0,21
0,26
0,31
Tensile strain [mm/mm]

Appendix V: Additional information about SEM

Scanning electron microscopy is a method which performs a surface scan of the sample utilizing an incident electron beam. The electron source. sample and lenses need to be in vacuum and the sample needs to be conductive in order to dissipate the inherent charge in the incident electrons. These electrons interact with the sample creating certain signals that are useful to get information about the surface and composition of the sample: secondary electrons. backscattered electrons (BSE) and characteristic X-rays. Signals are detected and can be used to create images that are displayed in the computer.

Secondary electrons are pull out from the sample when a part of the energy from the primary electron beam is transferred. They are non-directional electrons and have very low energy. but when they are located close to the sample surface. a SEM image can be created giving information on the surface morphology of the sample.

Backscattered electrons are the ones which change direction when being scattered by the sample surface. They are high-energy electrons and because materials with high density would create more BSE. they can be used to obtain information on the chemical composition.

Appendix VI: Detailed steps to proceed with the study of the behaviour of an IPMC actuator subjected to different voltages

1) Set the function generator to a constant frequency of 0.008Hz (to give a period of 125s).
2) Select square-wave as the signal to apply by the function generator.
3) Set the voltage amplitude to 2V. This will lead to a peak voltage of 1V to each polarity.
4) Adjust the laser to the tip of the sample and zero the reading before starting.
5) Select the acquisition time and Press “Start” in the computer program to start recording the laser readings.
6) Let the sample actuate for 5 full cycles.
7) Press “Stop” in the computer program to stop recording the laser readings.
8) Increase the supplied voltage by 2V.
9) Disconnect the function generator.
10) Save the data from the computer program in an Excel sheet
11) Wait 2 minutes until the next test to let the sample recover some humidity.
12) Repeat steps 4 to 11 until a value of 10V for maximum voltage is tested (20V voltage amplitude).

Appendix VII: Graphs for actuation of the IPMC of different thicknesses (0.09, 0.17 and 0.22mm) subjected to various voltages (from 1 to 10V)

- 0.09mm thickness:

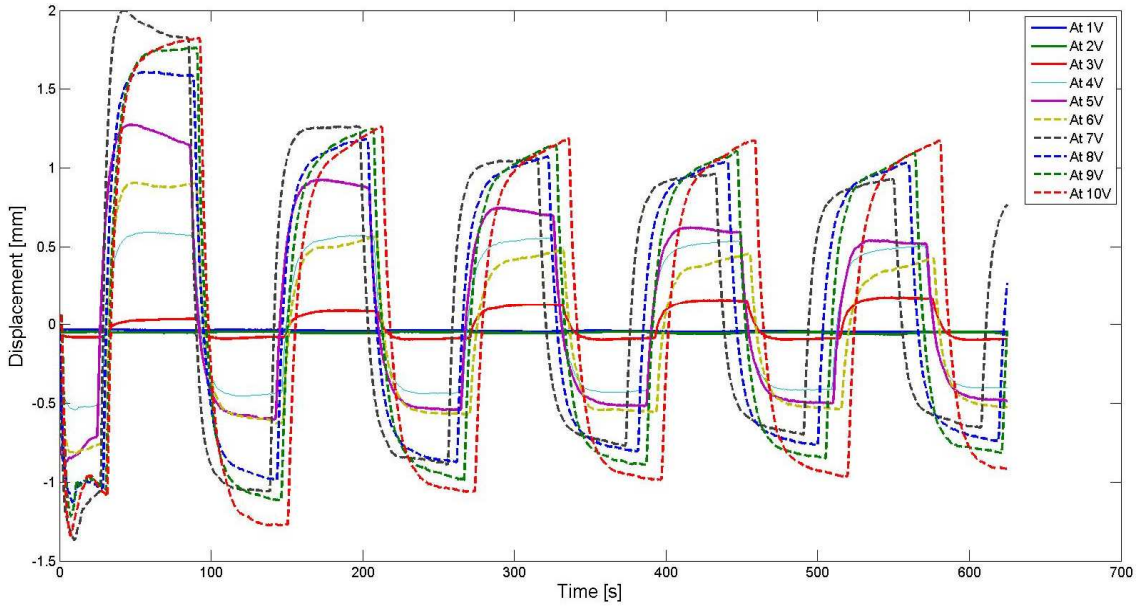

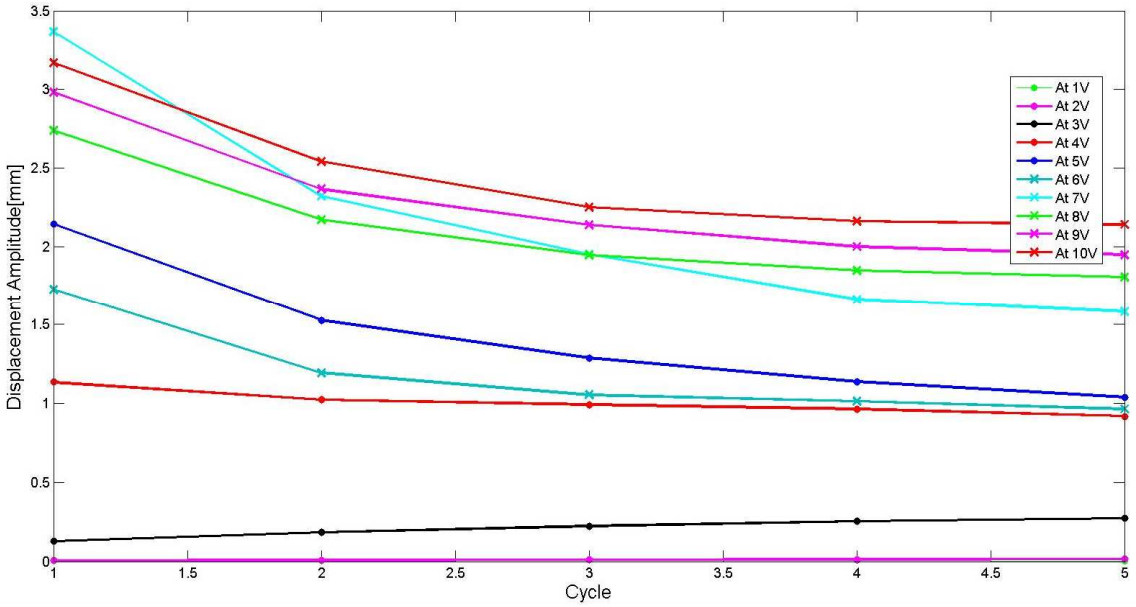

- 0.17mm thickness:

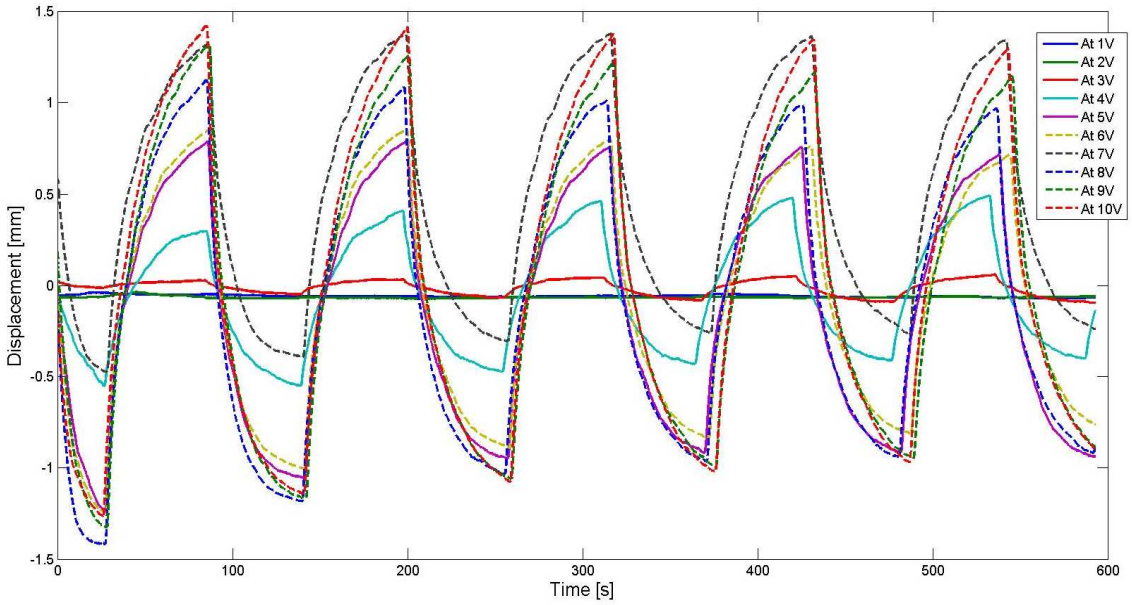

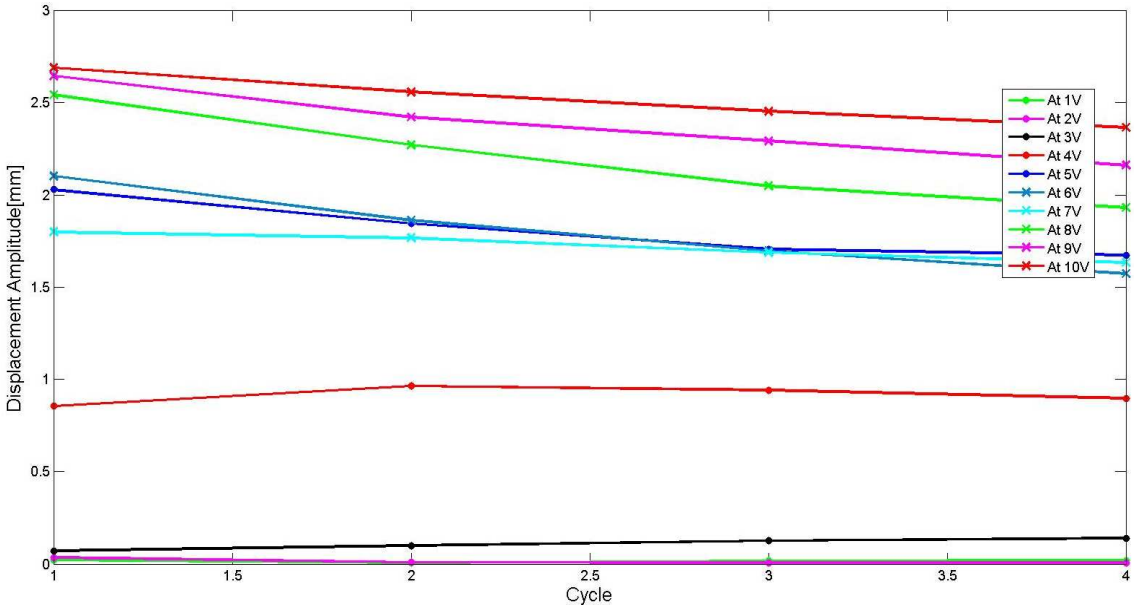

- 0.22mm thickness:

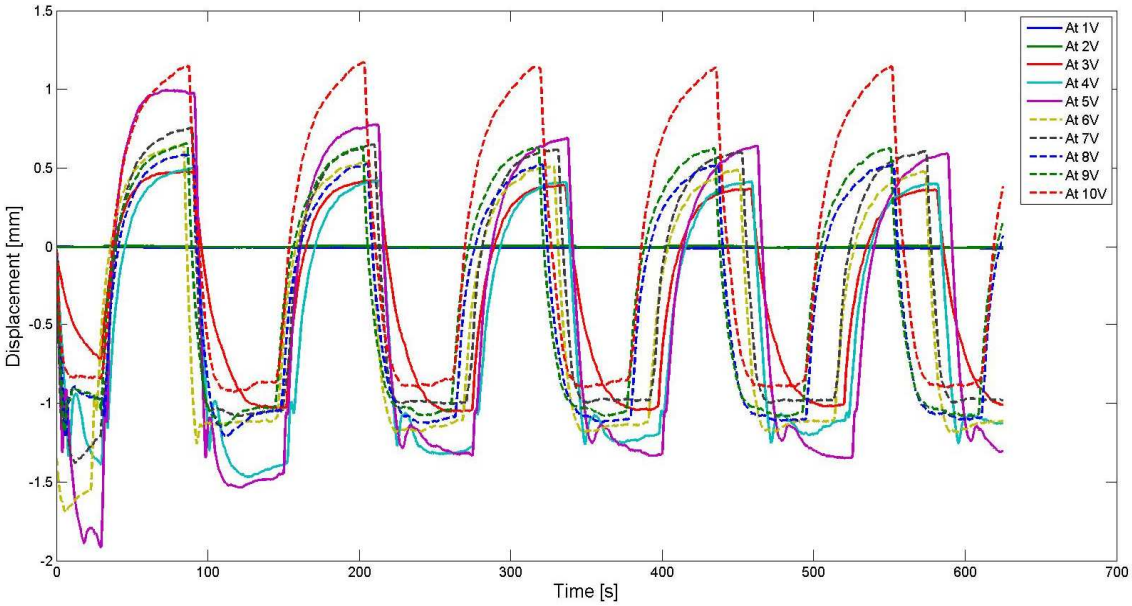

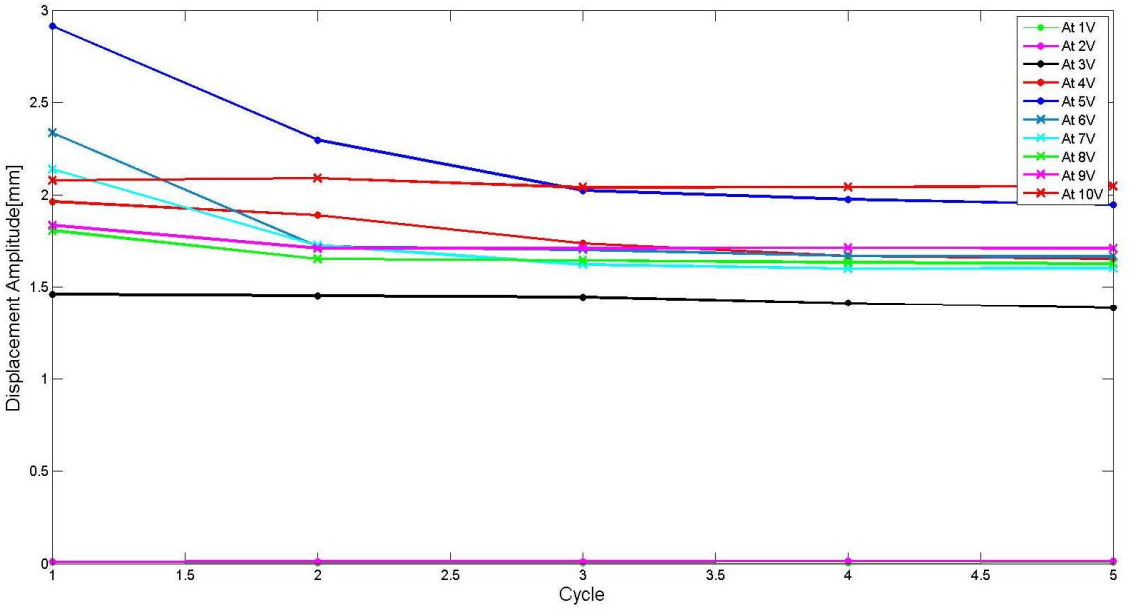

Appendix VIII: Detailed steps to proceed with the study of the behaviour of an IPMC actuator subjected to different frequencies

1) Set the function generator to a constant voltage amplitude of 10V (peak voltage of 5V).
2) Select square-wave as the signal to apply by the function generator.
3) Set the signal frequency to 0.001Hz.
4) Adjust the laser to the tip of the sample and zero the reading before starting.
5) Select the acquisition time and Press “Start” in the computer program to start recording the laser readings.
6) Let the sample actuate for 5 full cycles.
7) Press “Stop” in the computer program to stop recording the laser readings.
8) Increase the signal frequency.
9) Disconnect the function generator.
10) Save the data from the computer program in an Excel sheet.
11) Wait 2 minutes until the next test to let the sample recover some humidity.
12) Repeat steps 4 to 11 until a value of 500Hz.

Appendix IX: Graphs for actuation of the IPMC of different thicknesses (0.09 and 0.22mm) subjected to various frequencies (from 1 to 500mHz)

- 0.09mm thickness:

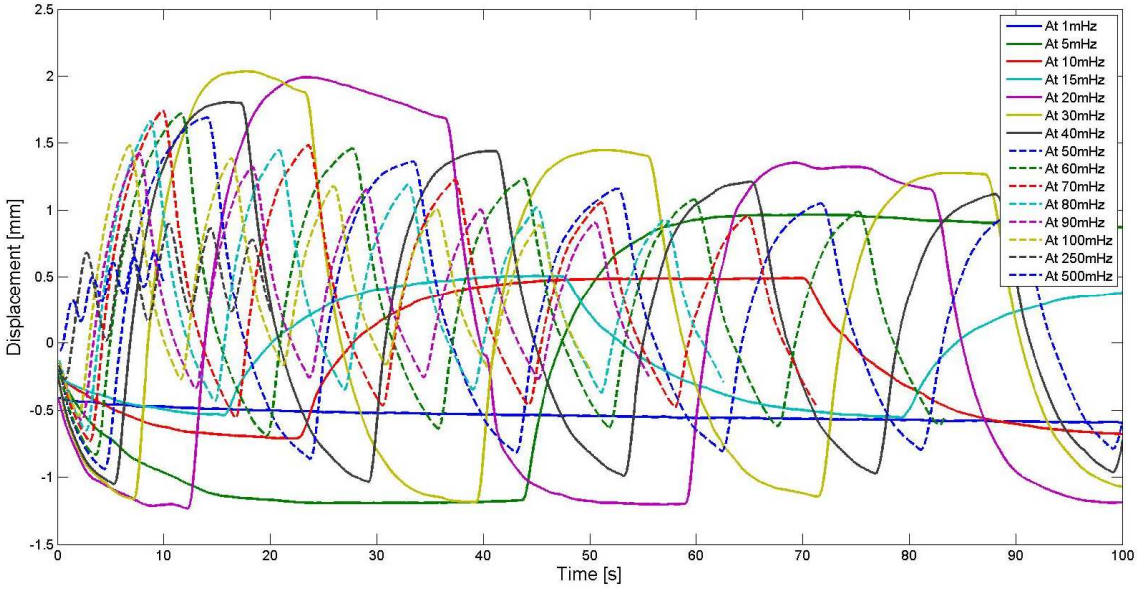

- 0.22mm thickness: